PROLINE SCANNING MUTAGENESIS OF SELECTED HELICES OF THE *Bacillus thuringiensis* Cry4B TOXIN

ISSARA SRAMALA

A THESIS SUBMITTED IN PARTIAL FULLFILLMENT OF
THE REQUIREMENTS FOR THE DEGREE OF
MASTER OF SCIENCE
(MOLECULR GENETICS-GENETIC ENGINEERING)
FACULTY OF GRADUATE STUDIES
MAHIDOL UNIVERSITY
1999

ISBN 974-662-707-4

Thesis

entitled

PROLINE SCANNING MUTAGENESIS OF SELECTED HELICES OF THE *Bacillus thuringiensis* Cry4B TOXIN

.....Issara Sramala.....

Mr. Issara Sramala
Candidate

.....

Assist. Prof. Chanan Angsuthanasombat, Ph.D.
Major-advisor

.....

Mr. Chartchai Krittanai, Ph.D.
Co-advisor

.....

Mr. Gerd Katzenmeier, Ph.D.
Co-advisor

.....

Prof. Liangchai Limlomwongse, Ph.D.
Dean
Faculty of graduate Studies

.....

Prof. Sakol Panyim, Ph.D.
Chairman
Master of Science Program in
Molecular Genetics and Genetic Engineering
Institute of Molecular Biology and Genetics

Thesis
entitled

PROLINE SCANNING MUTAGENESIS OF SELECTED HELICES OF THE *Bacillus thuringiensis* Cry4B TOXIN

was submitted to the Faculty of Graduate Studies, Mahidol University

for the degree of Master of Science (Molecular Genetics and Genetic Engineering)

on

28 May 1999

.....
Mr. Issara Sramala
Candidate

.....
Assist. Prof. Chanan Angsuthanasombat, Ph.D.
Chairman

.....
Prof. Sakol Panyim, Ph.D.
Member

.....
Mr. Chartchai Krittanai, Ph.D.
Member

.....
Mr. Namchai Chewawiwat, Ph.D.
Member

.....
Mr. Gerd Katzenmeier, Ph.D.
Member

.....
Prof. Liangchai Limlomwongse, Ph.D.
Dean
Faculty of graduate Studies

.....
Prof. Sakol Panyim, Ph.D.
Director
Institute of Molecular Biology and Genetics
Mahidol University

ACKNOWLEDGMENT

I wish to express my sincere thanks to my advisor, Assistant Professor Chanan Angsuthanasombat, for his warm guidance, dedicated efforts, valuable discussion and encouragement thoughout the course of this study and also my co-advisor and oral presentation committees Dr. Gerd Katzenmeier, Dr. Charchai Krittanai, Professor Sakol Panyim and Dr. Namchai Chewawiwat. I am greatly indebted to Dr. Albert for his kindly guidance, technical support and helpful discussion.

I am grateful to Mr. Panapat Uawithya and Mr. Umnaj Chanama for their helpful participant and valuable discussion.

This study was supported by Graduate Fellowship Program National Science and Technology Development Agency (NSTDA).

I would like to thank all scientist friends who participate the METHDS-REAGNTS and PROTEIN-ANALYSIS discussion groups at BIOSCI/bionet newsgroups for their kindly advice and sharing a valuable experience.

I am also indebted to my friends and all previous/present members of BDG group, and all technicians of the Institute of Molecular Biology and Genetics, Mahidol University who all share any success of this work.

Finally, I would like to express my deepest appreciation to my lovely parent, all members of my family, and all other friends for their patient, encouragement, and patronage. They are deserved to be mentioned as a part of my success.

Issara Sramala

4036160 STMG/M : MAJOR : MOLECULAR GENETICS AND GENETIC ENGINEERING ; M.Sc (MOLECULAR GENETICS AND GENETIC ENGINEERING)
KEY WORDS : DELTA-ENDOTOXIN, Cry4B, *Bacillus thuringiensis*, PORE-FORMATION, PROLINE SUBSTITUTION,

ISSARA SRAMALA : PROLINE SCANNING MUTAGENESIS OF SELECTED HELICES OF THE *Bacillus thuringiensis* Cry4B TOXIN. THESIS ADVISORS : CHANAN ANGSUTHANASOMBAT, Ph.D., CHARTCHAI KRITTANAI, Ph.D., GERD KATZENMEIER, Ph.D. 99 p. ISBN 974-662-707-4

The proposed mode of action of *Bacillus thuringiensis* (*Bt*) δ-endotoxins is the formation of lytic pores in the susceptible larval midgut epithelium. Recently published X-ray structures of two different Cry δ-endotoxins (Cry1Aa and Cry3A) revealed a possible apparatus for pore-formation in the form of a seven-amphipathic helix bundle in which five helices (α3, α4, α5, α6 and α7) are potential candidates for inserting into the membrane to form a transmembrane pore.

In this study, PCR-based mutagenesis was employed to investigate the role for toxicity of the putative transmembrane helices of the 130-kDa Cry4B mosquito-larvicidal toxin produced by *Bt* subsp. *israelensis*. Mutant toxins with a single proline substitution in the central region of α5, α6 and α7 were constructed on the basis of the homology based-Cry4B model, and were over-expressed in *Escherichia coli* as cytoplasmic inclusion bodies with a yield similar to that of the wild-type toxin. Unlike the wild-type inclusion, all proline-substituted inclusions were insoluble in carbonate buffer, pH 9.0, and gave no stable products when the solubilising buffer was supplemented with trypsin. A complete loss of larvicidal activity against *Aedes aegypti* larvae was also demonstrated for *E. coli* cells expressing mutant toxins in which residues Ala-182 or Leu-186 in α5, Tyr-220 or Ile-221 in α6, or Thr-254 or Val-257 in α7 were mutated. The results therefore suggest that these six residues might be involved in solubility and proteolytic susceptibility or toxicity of the Cry4B toxin.

4036160 STMG/M : สาขาวิชา : อณูพันธุศาสตร์และพันธุวิศวกรรมศาสตร์ : วท.ม. (อณูพันธุศาสตร์และพันธุวิศวกรรมศาสตร์)

คำสำคัญ : โปรตีนสารพิษ,Cry4B, *Bacillus thuringiensis*, การเกิดรูรั่ว, การแทนที่ด้วยโปรลีน

อิศรา สระมาลา : การเปลี่ยนแปลงกรดอะมิโนด้วยโปรลีนในเกลียวอัลฟาของโปรตีนสารพิษ Cry4B ผลิตจากแบคทีเรีย *Bacillus thuringiensis* (PROLINE SCANING MUTAGENESIS OF SELECTED HELICES OF THE *Bacillus thuringiensis* Cry4B TOXIN.). คณะกรรมการควบคุมวิทยานิพนธ์ : ชนันท์ อังศุธนสมบัติ, Ph.D., ชาติชาย กฤตนัย, Ph.D., GERD KATZENMEIER, Ph.D. 99 p. ISBN 974-662-707-4

กลไกการออกฤทธิ์ของโปรตีนสารพิษจากแบคทีเรีย *Bacillus thuringiensis* (*BT*) นั้นเชื่อว่าเกี่ยวข้องกับการเกิดรูรั่วที่ผนังเซลล์บุผิวกระเพาะอาหารส่วนกลางในแมลงที่กินสารพิษนี้เข้าไปซึ่งสอดคล้องกับข้อมูลจากโครงสร้าง 3 มิติของโปรตีนสารพิษ Cry1Aa และ Cry3A ที่ได้แสดงให้เห็นถึงส่วนของโครงสร้างที่ประกอบด้วยเกลียวอัลฟาที่เป็น amphipathic จำนวน 7 เส้น ซึ่งในจำนวนนี้มีเกลียวอัลฟา 5 เส้นที่คาดว่าสามารถสอดแทรกเข้าไปในผนังเนื้อเยื่อเพื่อทำให้เกิดรูรั่วได้

การวิจัยนี้ได้ศึกษาเกลียวอัลฟาที่คาดว่ามีความสัมพันธ์กับการเกิดรูรั่วของโปรตีนสารพิษ Cry4B ที่มีฤทธิ์ฆ่าลูกน้ำยุงจากแบคทีเรีย *Bt* subsp. *israelensis* โดยได้เปลี่ยนแปลงกรดอะมิโนในบริเวณกึ่งกลางเกลียวอัลฟาที่ 5, 6 และ 7 เป็นกรดอะมิโน proline โดยอาศัยวิธีการเปลี่ยนแปลงยีนเฉพาะที่ด้วยเทคนิคปฏิกิริยาลูกโซ่โพลีเมอเรส (PCR) ซึ่งได้สร้างโปรตีนกลายพันธุ์ที่ถูกออกแบบตามแบบจำลองโครงสร้าง 3 มิติของโปรตีนสารพิษ Cry4B หมด 6 ชนิดอันได้แก่ A182P และ L186P ซึ่งได้เปลี่ยนจาก alanine ที่ตำแหน่ง 182 และ leucine ที่ตำแหน่ง 186 ในเกลียวอัลฟาที่ 5 ไปเป็น proline, Y220P และ I221P ซึ่งได้เปลี่ยนจาก tyrosine ที่ตำแหน่ง 220 และ isoleucine ที่ตำแหน่ง 221 ในเกลียวอัลฟาที่ 6 ไปเป็น proline, T254P และ V257P ซึ่งได้เปลี่ยนจาก threonine ที่ตำแหน่ง 254 และ valine ที่ตำแหน่ง 257 ในเกลียวอัลฟาที่ 7 ไปเป็น proline ตามลำดับ เมื่อได้แสดงออกในแบคทีเรีย *Escherichia coli* พบว่าโปรตีนกลายพันธุ์ทั้ง 6 ชนิดถูกสร้างในรูปของก้อนผลึกโปรตีนภายในเซลล์เหมือนกับโปรตีนต้นแบบ (wild type) แต่ไม่สามารถถูกละลายได้ในสารละลายคาร์บอเนต pH 9.0 และไม่สามารถให้ชิ้นส่วนโปรตีนที่คงทนเมื่อถูกละลายในสารละลายคาร์บอเนตที่เติมด้วย trypsin นอกจากนี้เมื่อทดสอบความสามารถในการฆ่าลูกน้ำยุงลาย *Aedes aegypti* โดยใช้แบคทีเรีย *E. coli* ที่สร้างโปรตีนกลายพันธุ์แต่ละชนิดพบว่าโปรตีนกลายพันธุ์ทั้ง 6 ชนิดนี้ได้สูญเสียความสามารถในการฆ่าลูกน้ำยุง ผลการวิจัยนี้สามารถสรุปได้ว่ากรดอะมิโนที่ได้ถูกเปลี่ยนแปลงในตำแหน่งดังกล่าวข้างต้นในเกลียวอัลฟาที่ 5, 6 และ 7 มีความสำคัญต่อความสามารถในการละลายและความคงทนต่อการตัดย่อยด้วยเอนไซม์ trypsin ซึ่งมีผลกระทบโดยตรงต่อความเป็นพิษของโปรตีนสารพิษ Cry4B

CONTENTS

LIST OF TABLES

Table **Page**

LIST OF FIGURES

Figure **Page**

LIST OF ABBREVIATIONS

%(V/V)	Percent volume by volume
%(W/V)	Percent weight by volume
%(W/W)	Percent weight by weight
%C	Percent of crosslink
%T	Percent of Gel
Å	Angstrom.
Amp	Ampicillin
AU	Absorbency Unit
bp	base pair(s)
BSA	Bovine serum albumin
Bt	*Bacillus thuringiensis*
Bti	*Bacillus thuringiensis* subsp *israelensis*
°C	Degree celsius
ca	Approximately
cm	centimeter(s)
Cry	Crystal
Cyt	Cytolytic
DDT	Dithiothreitol
DNA	Deoxyribonucleic acid
DNase	Deoxyribonuclease
dNTPs	dATP, dCTP, dGTP, dTTP

E. coli	*Escherichia coli*
EDTA	Ethylenediaminetetraaceticacid
et al.	and others
EtBr	Ethidium bromide
g	gram(s)
μg	microgram(s)
hr(s)	Hour(s)
IPTG	Isopropyl-β-D-thiogalactopyranoside
kb	Kilobase(s)
kDa	Kilodalton(s)
μl	Microliter(s)
LB	Luria-Bertani medium
μm	Micrometer(s)
M	Molar
mA	MilliAmpare
mg	Milligram(s)
min	Minute(s)
ml	Milliliter(s)
mM	Millimolar
M_r	Relative molecular mass
N	Normal (concentration)
ng	Nanogram(s)
nm	Nanometer(s)

nmol	Nanomol
N-terminal	Amino terminal
OD	Optical density
p.s.i.	Pounds per square inch
PCR	Polymerase chain reaction
Rcf	Relative centrifugal force
Rnase A	Ribonuclease A
rpm	Revolutions per minute
SDS	Sodium dodecyl sulfate\
SDS-PAGE	Sodium dodecyl sulfate polyacrylamide gel electrophoresis
sec	Second(s)
subsp.	Subspecies
TEMED	*N, N, N′, N′*-tetramethylethylenediamine
Tris	Tri(hydroxymethyl)-aminomethane
U	Unit(s)
UV	ultraviolet
V	Volt

CHAPTER I

INTRODUCTION

1. General Background

Bacillus thuringiensis (*Bt*) is a Gram-positive soil bacterium. It is the most widely used environment-friendly alternative to chemical insecticides for the biological control of forest and agricultural pests and vectors of human and animal diseases. During sporulation, different strains of this bacterium produce larvicidal protein (delta-endotoxins) in large quantities as crystalline inclusions. These inclusions are composed of one or more toxins (Cry and/or Cyt toxins). The Cry (crystal) toxins (70-140 kDa) are highly toxic to different insect larvae (1, 2, 3) in the orders of Lepidoptera (butterflies and moths), Diptera (mosquitoes and flies) and Coleoptera (beetles). Cry proteins are also selectively toxic to nematodes, flatworms and protozoa (4). The 27-29 kDa Cyt (cytolytic) toxins show a wide range of cytolytic activity against insect and mammalian cells *in vitro* but only to dipteran larvae *in vivo* (1, 2). The Cry toxins can be classified according to their insecticidal activity spectra (2) and deduced amino acid sequence similarity (5) as illustrated in **Fig. 1**. The updated information of the delta-endotoxin nomenclature is available online (http://www.biols.susx.ac.uk/Home/Neil_Crickmore/Bt/index.html). For example, the 130-kDa Cry4B toxin which is produced by *Bt* subsp. *israelensis* and specifically toxic to the dipteran *Aedes sp.* and *Anopheles sp.* mosquito-larvae (2) is classified as Cry4Ba1. The complete *cry4B* gene sequence has been cloned (6) and referred as the genebank

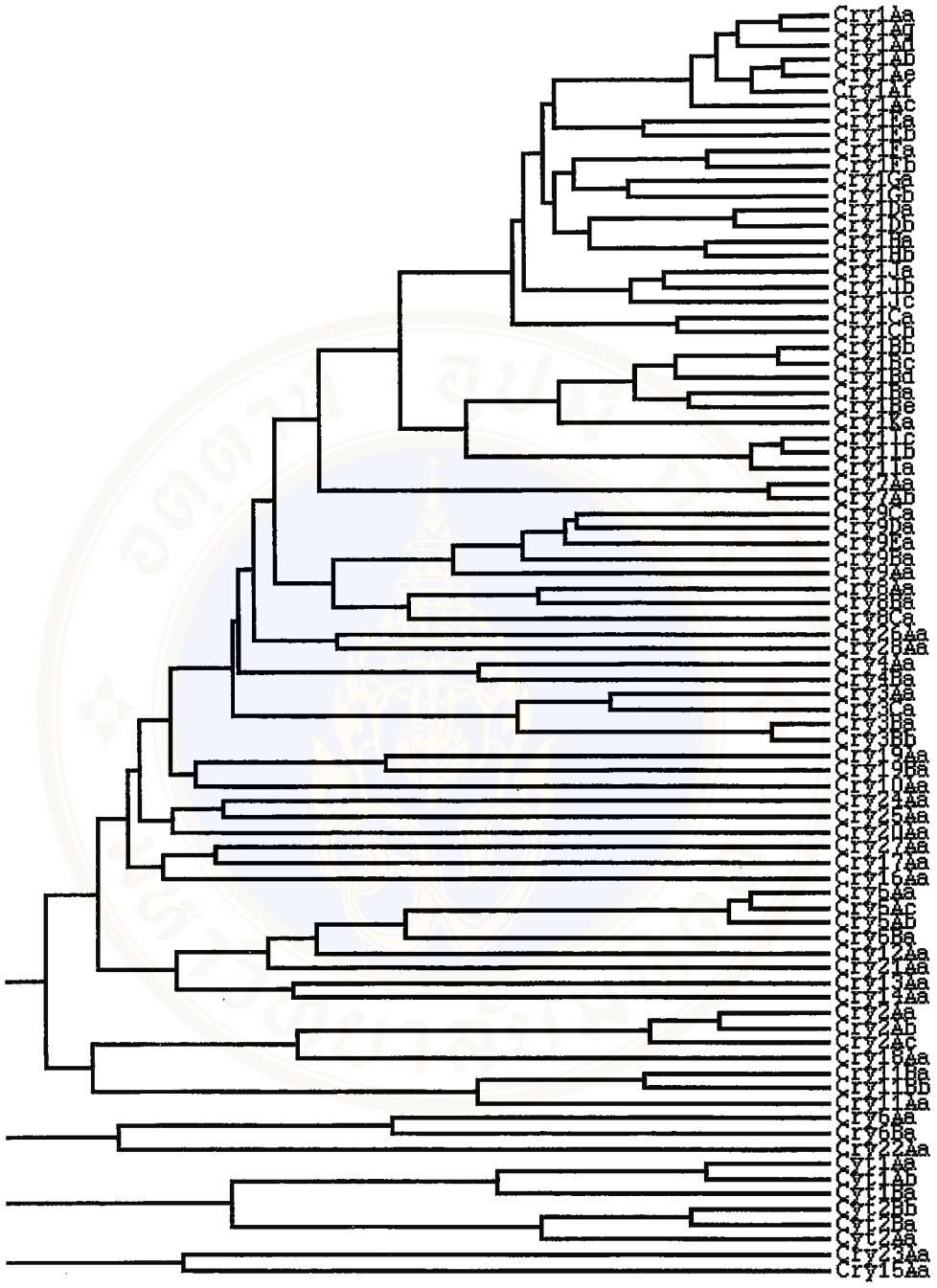

Fig. 1 : Phylogram demonstrating amino acid sequence identity among Cry and Cyt proteins.

This phylogenetic tree is modified from a TREEVIEW visualization of NEIGHBOR treatment of a CLUSTAL W multiple alignment and distance matrix of the full-length toxin sequences. The Phylogram was updated on 23/4/98. Last updated version can be accessed online at http://www.biols.susx.ac.uk/Home/Neil_Crickmore /Bt/index.html.

accession number of X07423 (7).

2. Protein Structure of Cry Toxins

Over 50 *cry* genes have been cloned and their sequences have been obtained (8). Based on the presence of five highly conserved regions in the deduced amino acid sequences of the Cry proteins, it was proposed that all Cry toxins will adopt a more or less similar tertiary structure (2). This postulate has been supported by the recently published crystal structures of the lepidopteran-specific Cry1Aa toxin (9) and the coleopteran-specific Cry3A toxin (10). Despite the differences in insect specificity and the comparatively low amino acid sequence identity (36%) between these two proteins, their structures display a high degree of overall similarity. Both molecules are composed of three distinct domains. Domain I is a seven-helix bundle in which the central helix (α-5) is relatively hydrophobic and surrounded by six amphipathic helices. This domain has been shown to be responsible for membrane insertion and pore formation (11, 12, 13, 14, 15). Domain II consists of three anti-parallel beta-sheets containing three surface-exposed loops. Reciprocal hybrid genes between Cry1Aa and Cry1Ac resulted in chimeric toxins with altered specificity (16, 17). Some mutagenesis data also confirmed that the loop region in domain II is involved in receptor binding (18, 19, 20, 21, 22, 23, 24, 25). Moreover, this domain is the most divergent part in the two toxin structures (9). It has been suggested to be involved in receptor recognition and hence determines insect specificity. Domain III is a tightly packed beta-sandwich of two anti-parallel sheets. The physiological function of this domain is still in debate although it has been suggested to be involved either in pore formation (26, 27) or in insect specificity through their involvement in specific

binding to insect gut epithelial receptors (18, 28, 29, 30, 31, 32). It has been demonstrated that domain III substitutions direct the binding of these toxins to different gypsy moth midgut receptors. Some reports have also suggested that the beta sandwich domain is critical for the structural integrity of the active Cry toxin by preventing the toxin from proteolytic degradation by gut proteases (10).

Based on amino acid sequence alignment of Cry1Aa, Cry3A and Cry4B (**Fig. 2**) it can be predicted that Cry4B would fold in the same manner as the two other toxins, especially at the N-terminal region of the molecule which is important for membrane insertion and pore formation (**Fig. 3, 4**).

3 Mechanism of Action of Cry Toxins

3.1 Solubilization and Proteolytic Activation

The mode of action of the insecticidal proteins is still a matter of investigation. Generally, the Cry toxins are present in the form of inactive protoxins as insoluble parasporal crystalline inclusions (2). Upon ingestion by susceptible larvae, the inclusions are solubilized in the alkaline pH in larval midgut. The solubilized protoxins are then cleaved *in vivo* by gut proteases to release active toxins. The toxin activation can be done *in vitro* by incubating the protoxins with larval gut extract or trypsin (3, 4). For example, some studies showed that the *in vitro* activation of the Cry3A toxin obtained from *Bt* subsp. *tenebrionis* 1911 yielded the ca. 65-kDa trypsin resistant protein (33).

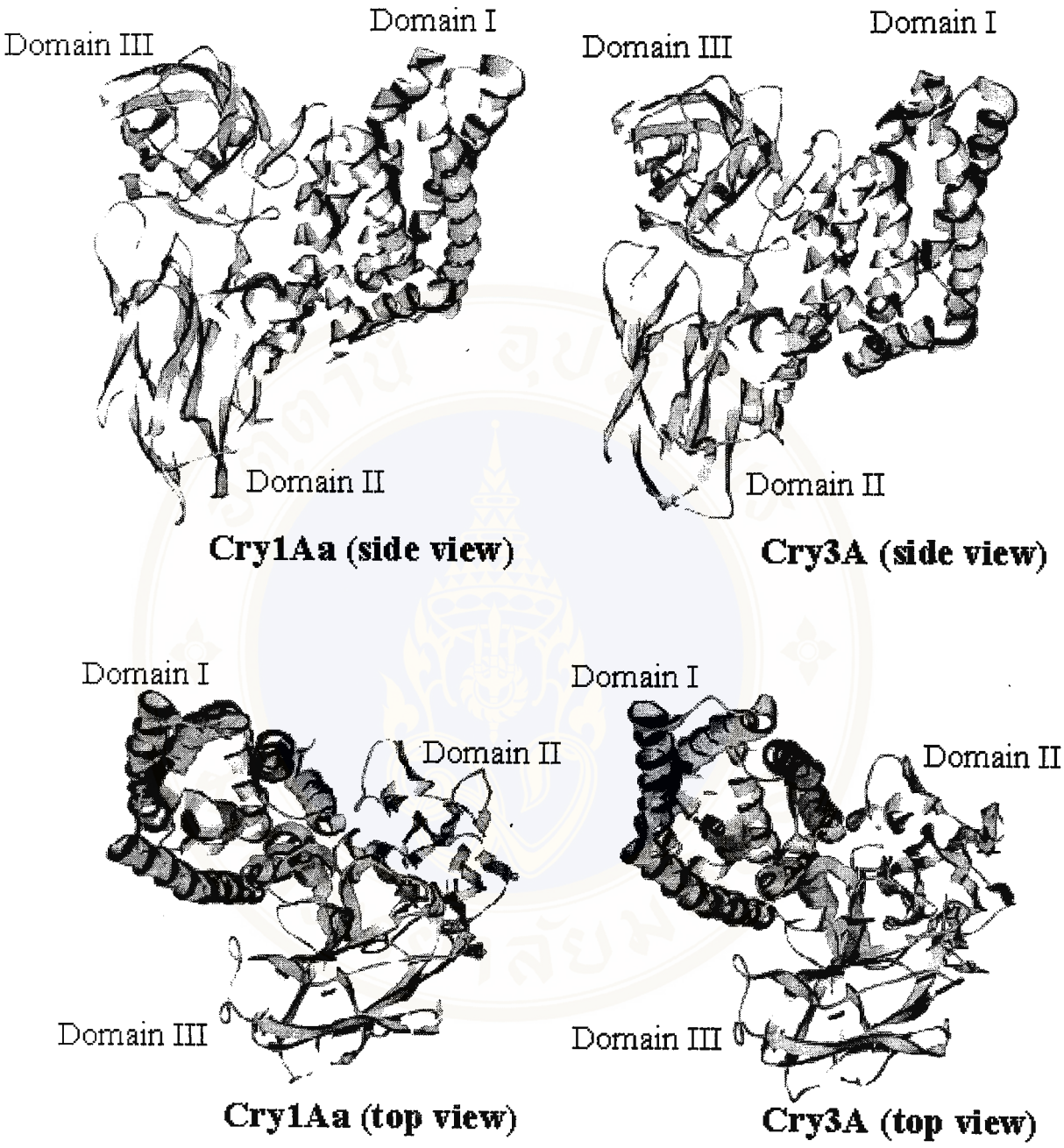

Fig. 3 : Ribbon models show the x-ray crystal structure of Cry1Aa and Cry3a
The figure show side and top view of two models which constructed from x-ray crystal structure data of Cry1Aa (9) and Cry3a (10).

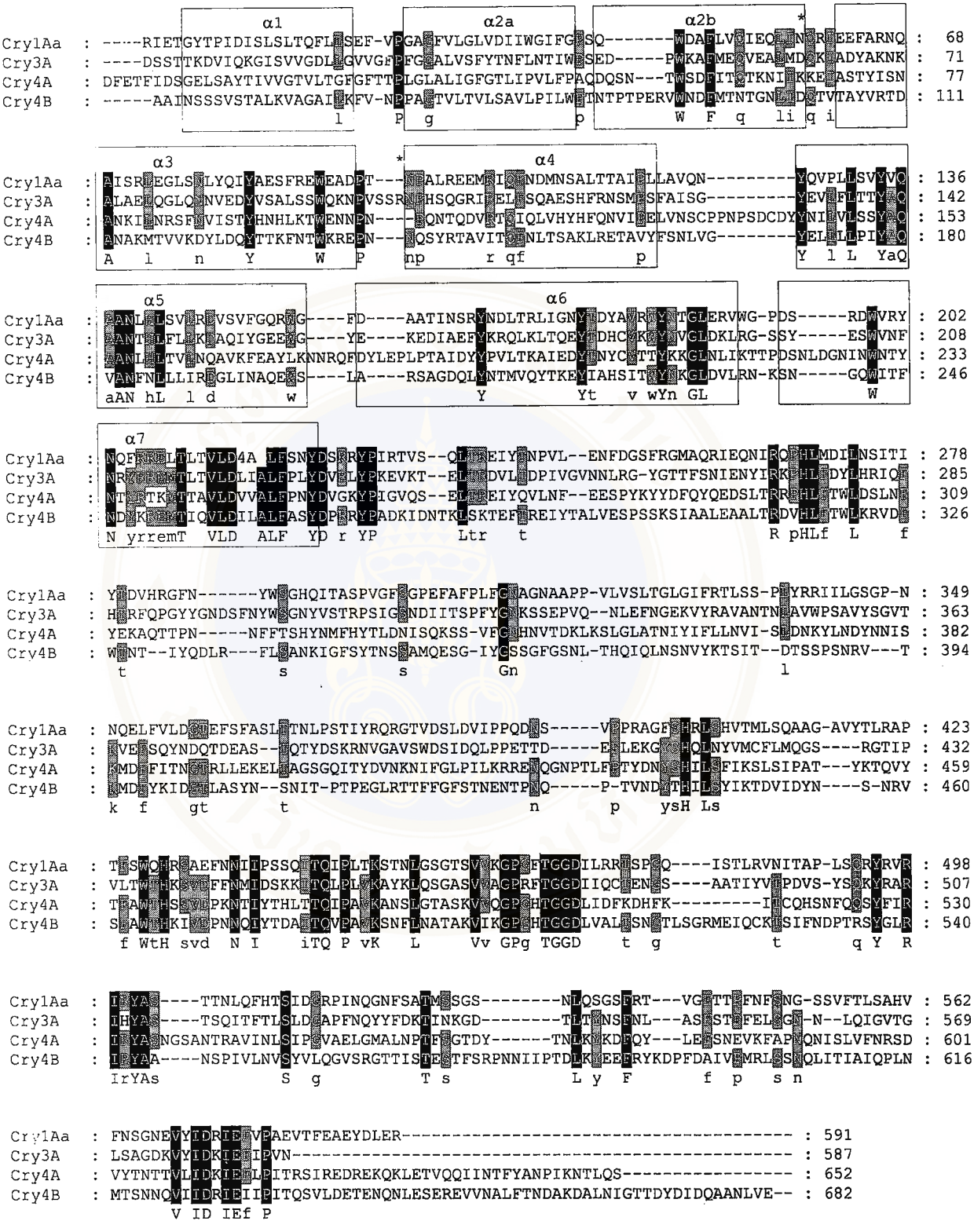

Fig 2 : Amino acid sequence alignments of Cry4-class toxins and its neighbors.

The figure shows aligned sequences of Cry4-class toxins and two known structures, Cry1Aa and Cry3A. The shaded letters represent conserved residues. Consensus sequence was lied below the aligned sequences. All alpha helices in domain I were marked by boxes.

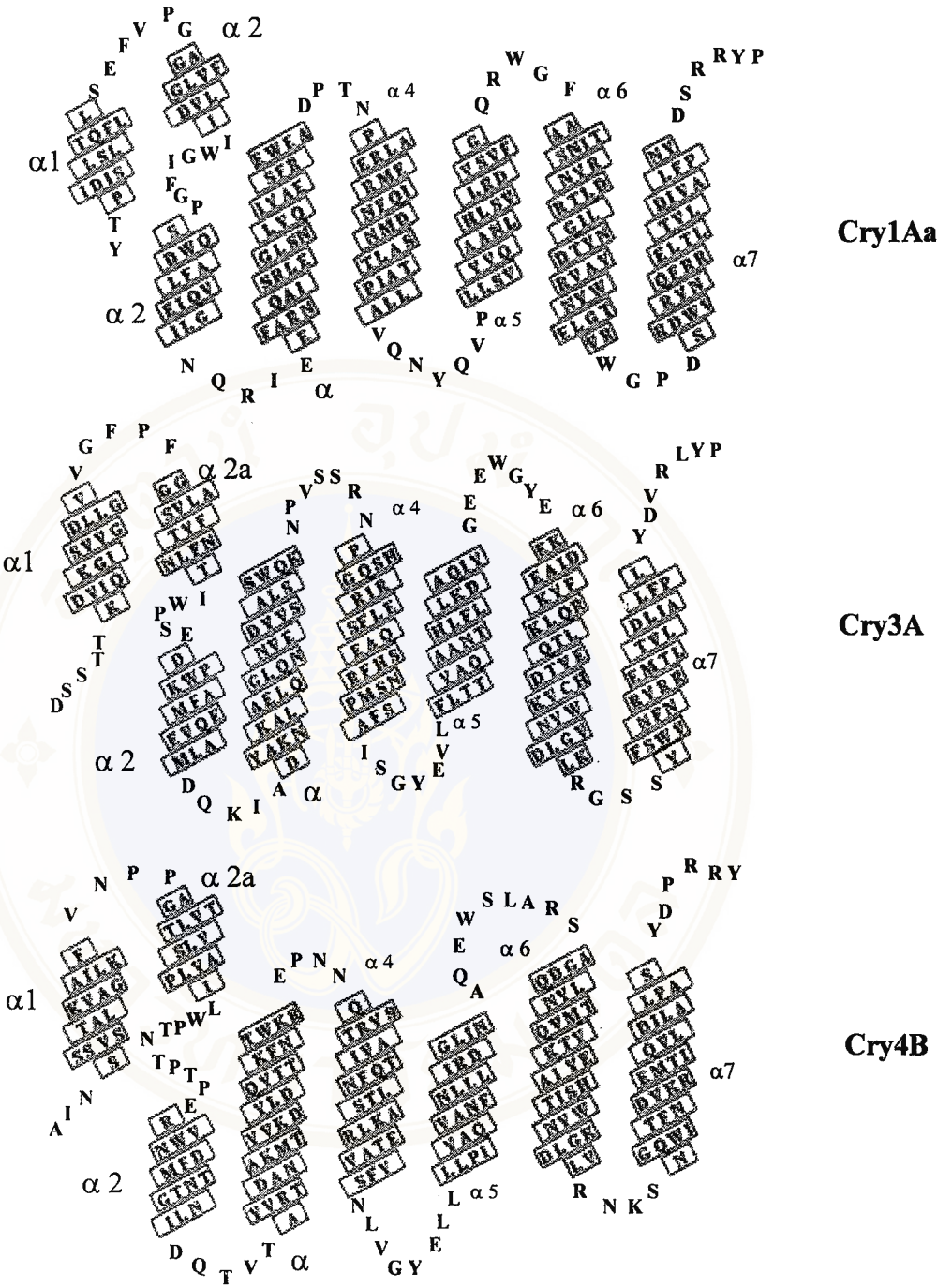

Fig 4 : Diagrams show seven-helix bundles of Cry1Aa, Cry3A and Cry4B

The structures of Cry1Aa and Cry3A are based on x-ray crystal structure and the structure of predicted Cry4B is based on sequence similarity.

3.2 Toxin-Receptor Binding

It is believed that the activated toxins first bind to a specific receptor in the luminal plasma membrane of midgut epithelial cells, leading to cell lysis and subsequent insect death by starvation or septicemia (1). In several studies for the binding ability of the Cry toxins have been carried out on brush border membrane vesicles (BBMV) (23, 24, 25, 30, 31, 32, 34, 35, 36). Two proteins were identified as delta-endotoxin specific receptors i.e. aminopeptidase-N and cadherin-like glycoprotein. The 100-kDa *Lymantria dispar* aminopeptidase-N has been identified as the unique Cry1Ac binding protein. The aminopeptidase-N clearly displayed strong binding to Cry1Ac but little or no binding to Cry1Aa or Cry1Ab. This protein also showed no binding for the coleopteran-specific toxin, Cry3A (37). The 170-kDa *Heliothis virescens* aminopeptidase-N is recognized by Cry1Aa, Cry1Ab and Cry1Ac, but not by Cry1C and Cry1E (38). The cadherin-like glycoprotein is a 210-kDa membrane glycoprotein that specifically binds the Cry1Ab toxin which is specific toxic for hornworm (39).

3.3 Toxin-Membrane Interaction and Oligomerization

After binding to specific receptors, the toxins insert into the membrane to form leakage pores. The loss of membrane integrity may cause the swelling and lysis via colloidal osmotic lysis (40) of insect gut cells.

The toxins, which are considered as cytolytic proteins, can disrupt cell membrane by several mechanisms: degrading the membrane component (41), disrupting the membrane by acting like surfactants (42) or forming a pore in the membrane (43, 44, 45). The formation of an ion channel or a pore was proposed to be

a lysis model for the Cry toxins. This proposal was postulated with colloidal osmotic lysis which resulted from ion flux through holes in lipid bilayers (11, 46, 47). There are two suggested models (1) suggested for the membrane inserting step. The first one is a the penknife model, which involves the flip out of helix-5 and helix-6 into the membrane like a penknife opening (see **Fig. 5**), and the second model is the umbrella model, which involves the insertion of helix-4 and helix-5 and the spanning of the other helices on membrane surface (see **Fig. 6**).

Villalon et al. (48) found that the pores formed by Cry1C allowed the diffusion of sucrose, but were impermeable to the trisaccharide raffinose. On the basis of the radii of these substances, the diameter of the pores was estimated to be 1.0-1.2 nm. The permiability of the pores observed in another experiment using raffinose (1.14 nm diameter) and non-electrolytes of increasing size were estimated to have a limiting diameter of approximately 2.4-2.6 nm under alkaline pH conditions (49).

Feng et al. (50) have studied Cry3A, Cry1Aa and Cry1Ac by means of size-exclusion and was found that the relative amounts of monomer and oligomer depended upon temperature, pH, and buffer composition. Guereca et al. (51) have reported that Cry1Aa, Cry1Ac, Cry1C, Cry1D and Cry3A toxins formed an oligomer consisting of more than ten units in both neutral and alkaline solution. It also suggested that oligomer formation might be a time-dependent process and might occur after the toxin binds to the receptor and inserts into the membrane.

Aronson et al. (52) examined the steps required for toxin insertion into the membrane and possible oligomerization to form a channel. When the Cry1Ab or Cry1Ac toxins were analyzed by immunoblotting, it was found that most of the toxins formed a large aggregate of ca. 200 kDa after incubation of the toxins with vesicles.

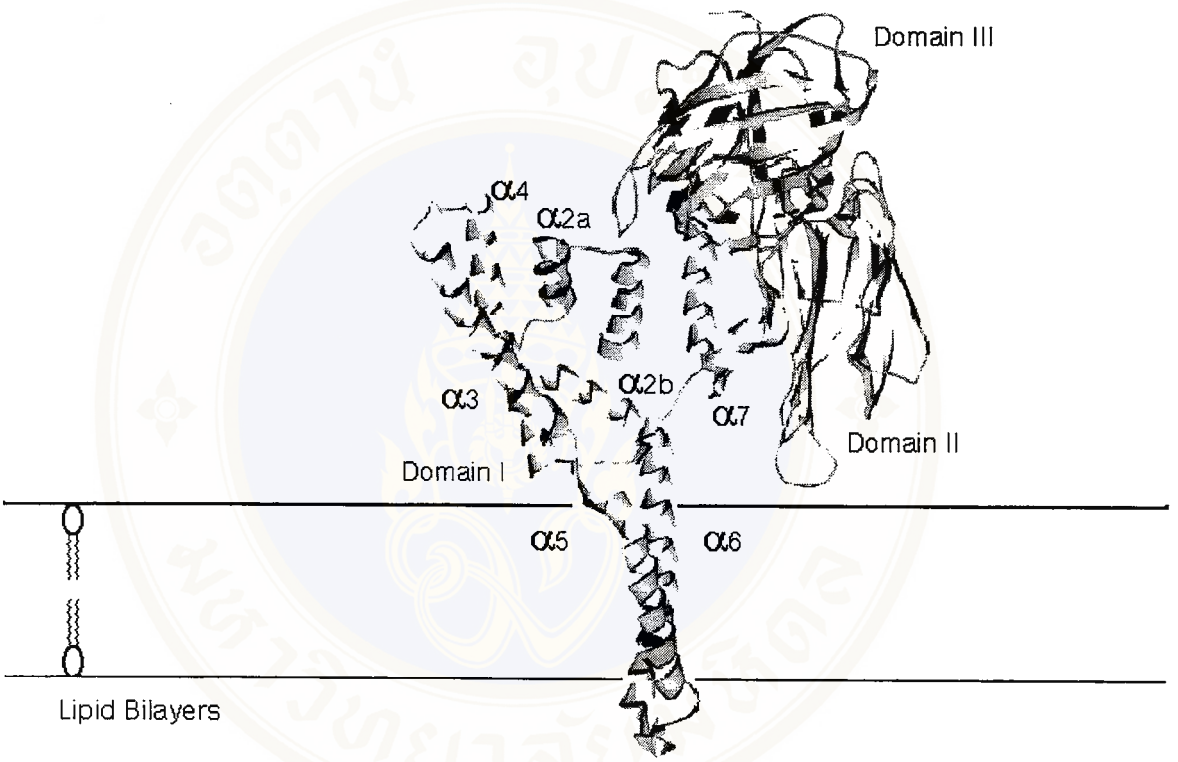

Fig. 5 : The penknife model

The figure shows the penknife model reproduced from Knowles (1). Helices 5 and 6 flip into the membrane as a helical hairpin.

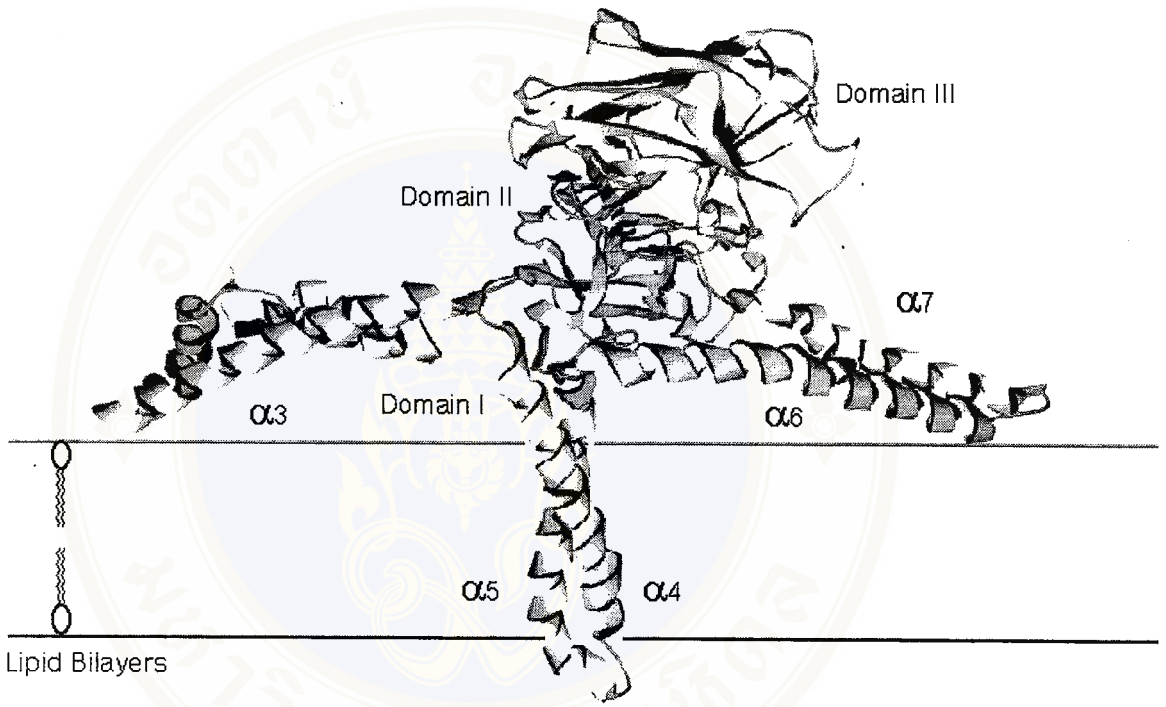

Fig. 6 : The umbrella model

The figure shows the umbrella model reproduced from Knowles (1). Helices 4 and 5 flip into the membrane as a helical hairpin.

No oligomerization occurred when mutant toxins with mutations in α 5 were tested. There was one exception; a very active helix 5 mutant toxin bound very well to membranes, but no oligomers were detected. Toxins with mutations in the loop connecting helices alpha 2 and alpha 3, which affected the irreversible binding to vesicles, also did not oligomerize.

3.4 Toxin-Ion Channel

The ion channel activity of Cry toxins has been explored by various techniques. The channel formation was first proposed by Knowles and Ellar (40) who reported the effect of Cry toxin on CF-1 cells and proposed the colloidal osmotic lysis model that caused by influx of water and ions resulting in cell swelling and lysis. Another proposal was presented by Harvey et al. (53) who found that Ba^{2+}, the K^+ channel blocking agent, could completely reverse *Bt* inhibition of the K^+-carried short circuit current in the isolated midgut of *Manduca sexta*. The suggestion of the cation selective channels was supported by demonstration of the effect of Cry1C, Cry3A Cry1Aa, Cry1Ab and Cry1Ac on the monovalent cation contents and intracellular pH of individual Sf9 cells (47). It was found that the toxins appeared to act specifically by increasing the permeability of the cytoplasmic membrane of susceptible cells to at least H^+, K^+ and Na^+ in time- and concentration-dependent manner. Peyronnet et al. (54) measured the effects of different toxins on the electrical potential of the apical membrane of freshly isolated midguts from *Lymantria dispar* and *Bombyx mori* larvae with a conventional glass microelectrode and reported that addition of toxins caused a rapid, irreversible, and dose-dependent depolarization of the membrane. They also suggested that the ability of Cry toxins to form pores in the midgut epithelial cell

membrane correlated with their *in vivo* toxicity. When the intracellular Ca^{2+} concentration was measured in single Cf1 cells loaded with a Ca^{2+}-sensitive fluorescent probe (55), Cf1 cells displayed Ca^{2+} surges in response to Cry1Ac and Cry1C proteins. They suggested that the toxins triggered intracellular Ca^{2+} surges which were mainly due to the influx of extracellular Ca^{2+} through toxin-made pores, as confirmed by planar lipid bilayer experiments.

Slatin et al. (42) showed that delta-endotoxins Cry1Ac and Cry3A could interact with receptor-free planar lipid bilayers and form ion-conducting channels. They suggested that channels formed by both toxins were cation-selective and that the toxicity of this toxin family may be caused by a common mechanism. In addition, Schwartz et al. (56) have reported that Cry1Aa, Cry1Ac and Cry1C could form channels in the receptor reconstituting planar lipid bilayers at much lower doses than in receptor-free membranes.

Schwartz et al. (57) have also demonstrated that the Cry1C toxin could penetrate into planar lipid bilayers and form ion-selective channels with a large range of conductances. These channels displayed complex activity patterns with subconducting states and were selective to either anions or cations. These properties appeared to be pH dependent. It was proposed that the effects of pH on the ion channel activity could be correlated with pH-dependent changes in secondary structure of these proteins. The secondary structure changes of the protoxin and toxin molecules at different pH values were previously observed by circular dichroism spectroscopy (58). The results showed that significant conformational differences were observed between the secondary structures of the protoxin and toxin molecules at different pH values. Moreover, Feng et al. (50) also studied Cry3A, Cry1Aa and Cry1Ac by means of circular dichroism

spectroscopy and reported that there was a significant increase in helical contents as the pH was changed from neutral to alkaline values, but no decrease at low pH.

It is believed that N-terminal fragment, especially domain I, being responsible for ion channel properties of the full length activated delta-endotoxin. The ion channel activity of this fragment has been observed with various Cry toxins.(44) showed that the proteolytically-derived amino-terminal fragments of Cry1Ac demonstrated ion channel activity in planar lipid bilayers and phosphatidylcholine vesicles. Von Tersch et al. (15) also showed that a cloned 7-alpha-helical bundle domain of Cry3b2 toxin was sufficient for ion channel formation and promoted ion efflux on phospholipid vesicles and black lipid membranes.

The role of the most conserved domain which located near the N-terminus has been investigated by site directed mutagenesis at several positions. Ahmad and Ellar (46) substituted two Asp residues located adjacent to each other in α-5 of this conserved segment of Cry1Ab with Phe and Val and suggested that regions close to the N-terminus of this helix could play an important role in the membrane insertion. Wu and Aronson, (47) also performed Ala-92 and Arg-93 mutations in α-5 of Cry1Ac and suggested that this amphipatic helical region of the toxin was essential for toxicity. The mutant toxins had lost the capacity to inhibit K^+-dependent amino acid transport into larval midgut vesicles, but there was no effect on their ability to compete with wild type toxin for binding. Chen et al. (14) also reported reduction of pore function observed for A92E and Y153D mutants of Cry1Ab as being tested by voltage clamping and irreversible binding to *Manduca sexta* brush border membrane vesicles. Hussain et al. (59) confirmed that substitution of a positively charged residue (R93F) or addition of a negatively charged residue (A92D) at the N-terminal of α 3 helix of

the Cry1Ac delta-endotoxin resulted in a substantial reduction in toxicity against *Manduca sexta*. However, replacing A119 in a loop on the distal side of the helices with negatively charged residues (A119D or A119E) did not affect toxicity or irreversible binding. The results support the model that domain I is involved in membrane integration and pore formation.

Disulfide bridge mutation in the domain I of CrylAa demonstrated that this helical domain was involved in membrane integration and permeation (11). They showed that unfolding of the protein around a hinge region linking domain I and II was a necessary step for pore formation. They also suggested that membrane insertion of alpha-helices 4 and 5 played a critical role in the formation of a functional ion channel. The proposal was supported by proline substitution mutagenesis on α-3 and α-4 (60). It was revealed that helix 4 of the Cry4B toxin could possibly involved in the membrane insertion and pore formation rather than in receptor recognition.

Roles of arginine in the conserved region in third domain were also determined via mutagenesis by Chen et al. (27). They converted residues 525-535 of Cry1Aa to other residues and reported that the toxins, which were mutated to replace lysine for the first and fourth arginines, were unaltered in expression and structure but were substantially reduced in their insecticidal properties and inhibition of short circuit current across *Bombyx mori* midguts. It was proposed that this region played a role in toxin function as an ion channel. The proposal was supported with two other mutagenesis experiments. Wolfersberger et al. (61) replaced the first, second, and last arginine residues of the conserved third-domain sequence, R-521 YRVRIR-527, with other amino acids. The stable mutant proteins were bioassayed against *Bombyx mori* larvae and were found to be approximately half as active as wild-type CryIAa. The

toxins were also tested by means of a light-scattering assay for their ability to increase permeability of larval *B. mori* midgut brush border membrane vesicles. The study performed by Schwartz et al. (26) has provided the first direct evidence of a functional role for domain III in membrane permeabilization. They have studied on five Cry1Aa mutants which were constructed by replacing Arg-521 by Lys (R521K), Gln (R521Q), His (R521H), or Glu (R521E) and Arg-527 by Lys (R527K). It was suggested that residues of the positive arginine face of block 4 interact with domain I, the putative pore-forming region of Cry1Aa.

Some of amphipathic helices were studies by using synthetic peptides as the model. Cummings et al. (45) studied on a synthetic 31-mer peptide corresponding to the sequence of the central helix (α 5) of CrylAc on structural and functional properties. It was found that the peptide could exist as an alpha-helix in methanol and as a random coil in water. In addition, the peptide could associated with liposomes at pH 4.7 and formed channels in planar lipid bilayers.

Gazit and Shai (62) synthesized the peptide corresponding to the α 5 segment, amino acid residues 193-215 of Cry3A and its proline incorporated analogue (P-α 5), and selectively labeled at their N-terminal amino acids with fluorescent probes. It was reported that α 5 was much more active than P-α 5. The same approach was used in characterization of the ability to self-assemble and to co-assemble within lipid membranes of α 5 and α 7 (63). It was revealed that, in their membrane-bound state, α 5 could self-associate but α 7 could not, and that α 5 could coassembles with α 7 but not with an unrelated membrane bound α-helical peptide.

Gazit et al. (64) also investigated the role of α-5 with respect to its interaction with Sf-9 cell membranes and its propensity to form ion channels in planar lipid

membranes. Functional characterization of α-5 has revealed that it was cytotoxic to Sf-9 insect cells, and could form ion channels in planar lipid membranes. Moreover a proline-substituted analogue of α-5 was less cytolytic and slightly more exposed to enzymic digestion. These findings would support a role for α-5 in the mechanism of the delta-endotoxins, as one of the transmembrane helices to form the toxic pore.

Recently, Gazit et al. (12) have used resonance energy transfer measurements of all possible combinatorial pairs of membrane-bound helices to map the network of interactions between helices in their membrane-bound state. It was proposed that α-4 and α-5 would insert into the membrane as a helical hairpin in an antiparallel manner, while the other helices would lie on the membrane surface like the ribs of an umbrella (the "umbrella model"). They also suggested that α-7 may serve as a binding sensor to initiate the structural rearrangement of the pore-forming domain.

CHAPTER II

OBJECTIVES

Although the structures of the Cry toxins have provided some insights into the possible steps leading to cell death, the identity of the membrane-inserting components in ion channel formation is still not clearly elucidated. Several studies with the isolated domain I of Cry1Ac (44) and Cry3B2 (15) and with synthetic peptides of helix-5 from Cry1Aa (9), Cry1Ac (45) demonstrated pore forming activity of in phospholipid bilayers.

A number of experiments including site-directed mutagenesis, synthetic peptides and computer simulation (12, 45, 46, 47, 62, 63, 64, 65) suggested that helix-5 is involved in pore formation. In addition to this central helix, four other amphipathic helices (helix-3, helix-4, helix-6 and helix-7) are longer than 30 Å thus capable of spanning the membrane and therefore could putatively be part of the transmembrane pore forming apparatus. Experiments using disulfide bond engineered mutants of Cry1Aa (11) indicated that membrane insertion of helices 4 and 5 in domain I plays a critical role in the formation of a functional pore. Recent studies of helix-3 and helix-4 of the Cry4B toxin also shown that helix-4 plays a role in membrane insertion and pore formation whereas helix-3 apparently did not participate in this function (60).

In this study, it was aimed to analyze further the possible involvement of helix-5, helix-6 and helix-7 in the pore forming process by constructing a number of proline substitution mutants for the Cry4B toxin. Proline substitution mutagenesis would lead

to structural and functional distortion of trans-membrane helix (60, 62) without significantly influencing the other helices or the overall topology (66).

CHAPTER III

MATERIALS

1. Chemicals

All chemicals used were analytical grade purchased from various suppliers (BIO-RAD, Fluka, Merck and Sigma) except for those specifically indicated.

2. Enzymes and Accessory Buffers

*Dpn*I	Promega
*Hha*I	Biolabs
*Hin*fI	Biolabs
*Hpa*II	Boehringer
Pfu (Native)	Promega
*Sau*96I	Biolabs
*Xba*I	Gibco BRL

All other enzymes used were purchased from Boehringer Mannheim, Gibco BRL, New England Biolabs, Promega, and Stratagene. The accessory buffers were supplied by the enzyme manufacturer.

3. Bacterial Strains

E. coli strain JM109 [*recA*1 *supE*44 *endA*1 *hsdR*17 *gyrA*96 *rclA*1 *thi*Δ(*lac-pro AB*) F′ (*traD*36 *proAB*$^{+}$ *lacI*^{q} lac*Z* ΔM15)] was purchased from Promega.

4. Vectors and Recombinant Plasmids

pMU388 (6) : a recombinant plasmid containing the 130 kDa Cry4B toxin gene (GenBank accession number : X07423 (7)) was used as DNA template for site directed substitution on putative pore forming region.

pUC12 : a cloning vector providing selection with Amp. (GenBank accession number : L09129) was used as vector-alone control.

5. Synthetic Oligonucleotides (Primers)

Synthetic oligonucleotides served as primers in PCR were synthesized by Bio-synthesis, U.S.A. for L186PF, L186PR, Y220PF, Y220PR, T254PF and T254PR and by oligonucleotide synthesis division of Central Equipment Laboratory, Mahidol university for A182PF, A182PR, I221PF, I221PR, V257PF and V257PR. The oligonucleotide sequences are shown as followed. The boldface letters indicate mutated nucleotide or amino acid residues. Introduced restriction endonuclease recognition sites are shown as underlined letters. Deduced amino acid sequences are shown above all forward primer sequences. Sequencing oligonucleotide, Q149PF was kindly supplied by Mr. Panapat Uawithya (60).

P I Y A Q V **P** N F N L

A182PF 5′ CCAATATACGCACA**G**GT**CC**CAAATTTCAATTTAC 3′

A182PR 5′ GTAAATTGAAATTTG**GG**AC**C**TGTGCGTATATTGG 3′

*Sau*96I

A N F N **P** L L I R D G L

L186PF 5′ GCAAATTTCAAT**CC**ACTTTTAAT**CC**G**G**GATGGCCTC 3′

L186PR 5′ GAGGCCATC**CC**G**G**ATTAAAAGT**GG**ATTGAAATTTGC 3′

*Hpa*II

Y T K E **P** I A H S I T W

Y220PF 5′ GTACACTAAAGAA**CC**TATTGC**G**CATAGCATTACATGG 3′

Y220PR 5′ CCATGTAATGCTATG**C**GCAATA**GG**TTCTTTAGTGTAC 3′

*Hha*I

T K E Y **P** A H S I T W

I221PF 5′ CACTAAAGAATAT**CC**TGC**G**CATAGCATTACATGG 3′

I221PR 5′ CCATGTAATGCTATG**C**GCA**GG**ATATTCTTTAGTG 3′

*Hha*I

D T K R E M **P** I Q V L

T254PF 5′ GATTATAAAAGAGAGATG**CC**G**G**ATTCAAGTATTAG 3′

T254PR 5′ CTAATACTTGAAT**C**G**G**CATCTCTCTTTTATAATC 3′

*Hinf*I

E M T I Q **P** L D I L A

V257PF 5′ GAGATGACTATTCAA**CCTC**TAGATATACTCGCTC 3′

V257PR 5′ GAGCGAGTATATCTA**GA**G**G**TTGAATAGTCATCTC 3′

*Xba*I

6. Miscellaneous

BIO-RAD Protein Assay	BIO-RAD
Standard DNA marker	Gibco BRL, Biolabs
SDS-PAGE molecular weight standards, broad range	BIO-RAD

CHAPTER IV

METHODS

1. Construction of Cry4B Mutants

1.1 Extraction of Plasmid DNA Template Using the CTAB Method

A single colony of bacteria was inoculated in 3 ml LB broth [1%(w/v) casein hydrolysate, 0.5%(w/v) bacto-yeast extract, 0.5%(w/v) NaCl] containing 100 µg/ml ampicillin and incubated at 37°C with 200 rpm shaking for 16-20 hrs. Cell pellets were harvested in 1.5 ml microfuge tubes by centrifugation at 10,000 rpm for 30 sec and then resuspended in 200 µl of STET buffer (8%sucrose, 5% Triton X-100, 50 mM EDTA, 50 mM Tris-HCl, pH 8.0). To the cell mixture was added 10 µl of freshly prepared lysozyme solution (10 mg/ml) and incubated at room temperature for 20 min. Then, the mixture was boiled for exactly 30 sec and immediately centrifuged at 12,000 rpm for 15 min at room temperature. The pellet (chromosomal DNA) was removed with a sterile toothpick. Plasmid DNA and residual low molecular weight RNA were recovered from the supernatant by adding 1/10 volume of 5% CTAB. The contents were inverted 5-6 times and centrifuged at 12,000 rpm for 10 min at room temperature. The pellet was resuspended in 300 µl of 1.2 M NaCl by vigorous vortexing and 10 µl of RNase was added, inverted and incubated at 37°C for 30 min. The protein was removed by adding equal volume of chloroform, inverted vigorously and centrifuged at 12,000 rpm for 5 min at room temperature. The clear aqueous phase was transferred

to new tube. The DNA pellets were precipitated with 2 volumes of absolute ethanol at -80°C for 5 min and centrifuged at 12,000 rpm for 2 min at room temperature. The final DNA pellets were washed in 70% ethanol, dried and resuspended in 10 µl distilled water.

1.2 *In vitro* Proline Substitution Site Directed Mutagenesis

The recombinant plasmid pMU388 contains the full length of the *cry4B* gene which was cloned from *Bacillus thuringeinsis* subsp. *israelensis* into pUC12 vector. In order to substitute alanine-182, luecine-186, tyrosine-220 isoleucine-221, threonine-254 and valine-257 by proline. Six pairs of complementary oligonucleotide were designed and synthesized. Mutagenesis protocol was modified from the Quickchange mutagenesis kit 's instruction (Stratagene).

The target DNA fragments were amplified by polymerase chain reaction by using pMU388, the plasmid which carries the complete *cry4B* gene as PCR template. *Pfu* DNA polymerase (Stratagene) was employed to achieve the highest fidelity. All primer sequences are shown in **CHAPTER III.**

A182PF and A182PR mutagenesis primers were used for construction of pA182P, a plasmid DNA which codes for a proline substitution in α5. L186PF and L186PR mutagenesis primers were used for construction of pL186P, a plasmid DNA which codes for a proline substitution in α5. Y220PF and Y220PR mutagenesis primers are used for construction of pY220P, a plasmid DNA which codes for a proline substitution in α6. I221PF and I221PR mutagenesis primers are used for construction of pI221P, a plasmid DNA which codes for a proline substitution in α6.

T254PF and T254PR mutagenesis primers are used for construction of pT254P, a plasmid DNA which codes for proline substitution in α7. V257PF and V257PR mutagenesis primers are used for construction of pV257P, a plasmid DNA which codes for proline substitution in α7.

1.3 Setting Up and Cycling the PCR Reactions

A GeneAmp®PCR System 2400 (Perkin Elmer Cetus) was used for controlled incubation of PCR-samples. The PCR reactions of the mutants were performed by using material informed in Stratagene 's Quick Change™ Site-directed Mutagenesis Kit.

The PCR reaction mixture (50 µl) composition is as follows:

pMU388	100 ng
dNTP	50 µM each
Forward and Reverse primers	10 pmole each
10x Native *Pfu* buffer	5 µl
Native *Pfu* DNA polymerase	2.5 U

Following the temperature cycle, the PCR products were examined on 0.8% agarose gels.

1.4 Agarose Gel Electrophoresis of DNA

To analyze the size or restriction pattern of DNA sample, the sample was subjected to agarose gel electrophoresis as described by Sambrook et al. (67). The appropriate amount of agarose powder (Prona) was dissolved in 1xTBE buffer [90 mM

Tris, 90 mM boric acid, 2 mM EDTA (pH 8.0)] under boiling temperature to insure the homogeneity of gel solution. When the gel mixture cooled down to about 60°C, the mixture was poured into the mold and allowed to cool and to solidify at room temperature. DNA sample solution was mixed with gel-loading dye [15%(w/v) Ficoll 400, 0.01%(w/v) Bromophenol blue] at ratio 1:5 and loaded into the well of the gel.

The electrophoresis was performed at constant voltage of 100 V in the same buffer that was used to prepare the gel. After the electrophoresis was completed, the gel was stained in 0.5 μg/ml ethidium bromide solution for 5-10 min and then destained in single distilled water for 10-15 min. The DNA band was visualized under UV.

1.5 Preparation of Competent *E. coli*

The method for preparation of competent *Escherichia coli* was described by Sambrook et al. (67). A single colony of *E. coli* strain JM109 was cultured in 3 ml of LB broth at 37°C with 250 rpm shaking for 16-20 hrs. The overnight culture was transferred into fresh LB broth at 1:100 dilution and incubated at 37°C with 250 rpm shaking until AU_{600} is 0.25-0.5. After the culture was chilled on ice for 15 min the *E. coli* was centrifuged at 2500 rpm for 15 min at 4°C. The pellet was gently resuspended in one-third the original volume in cold 0.1 M $CaCl_2$, incubated on ice for 1 hr and then centrifuged at 3,000 rpm for 15 min at 4°C. The *E. coli* pellet was gently resuspended in cold 0.1 M $CaCl_2$ and incubated on ice for 15 min. The competent *E. coli* mixture was aliquoted into microcentrifuge tubes and stored at -80°C until required. The efficiency of the prepared competent cell was determined by

transforming of 10 ng of pUC12 into 100 µl of the prepared competent *E. coli* cell suspension.

1.6 Digesting the PCR products

To each amplified reaction was added 1 µl of *Dpn*I restriction endonuclease, gently and throughout mixed and incubated at 37°C for 1 hour. The *Dpn*I will digest the parental *i.e.* nonmutated methylated or hemimethylated dsDNA. Then, 15 µl of the *Dpn*I digested PCR products were analyzed on a 0.8% agarose gel.

1.7 Transformation of *E. coli*

The transformation of *E. coli* was based on the protocol described in the U.S.E. Mutagenesis Kit Instructions (XY-042-00-04, Rev.2) from Pharmacia Biotech with some modification.

An aliquot of 100 µl of competent *E. coli* was mixed with the solution of DNA to be transformed. The cells were incubated on ice for 30 min, followed by incubation at 42°C for 45 sec, and then immediately chilled on ice for 2 min. 900 µl of 37°C LB broth were added to the transformed cells, and incubated at 37°C for 1 hr. The transformed cells were pelleted by centrifugation at 6,000 rpm for 1 min. The cells were spread on a LB agar plate containing 100 µg/ml ampicillin and incubated at 37°C for 16 hrs or until *E. coli* colonies were observed on the plate.

1.8 Plasmid Extraction

Plasmid extraction was performed with some modification of the Modified Mini Alkaline-Lysis described in Taq DyeDeoxy™ Terminator Cycle Sequencing Kit Manual (Part Number 901497) from Applied Biosystems.

E. coli culture was incubated overnight at 37°C in LB broth [1%(w/v) casein hydrolysate, 0.5%(w/v) bacto-yeast extract, 0.5%(w/v) NaCl], instead of Terrific Broth, with 100 μg/ml of ampicillin (67). 1.5-4.5 ml of cell culture was centrifuged at 10,000 rpm for 1 min in a microcentrifuge tube. The supernatant was removed and the bacterial pellet was resuspend in 200 μl of GTE buffer [50 mM glucose, 25 mM Tris-HCl (pH 8), 10 mM EDTA (pH 8)]. 300 μl of freshly prepared 0.2 M NaOH / 1%(w/v) SDS was added and the content was mixed by inversion, and incubated on ice for 5 min. 300 μl of 3.0 M potassium acetate pH 4.8 was added mix by inverting the tube, and incubate on ice for 5 min. Cellular debris was removed by centrifuging for 10 min at room temperature, and then transfer the supernatant to a clean tube. Unless other specified, the centrifugation in this study are preformed with Centrifuge 5415C (Eppendorf) in rotor F-45-18-11 (Eppendorf)

In order to remove RNA , RNase A (DNase free) was added at a final concentration of 20 μg/ml and the tube was incubated at 37°C for 20 min. The supernatant was extracted once with 400 μl chloroform. The solution was mixed by hand for 30 sec after each extraction. The tube was centrifuged for 1 min to separate the phases and remove the aqueous phase to a clean tube.

The total DNA was precipitated by adding an equal volume of 100% isopropanol and immediately centrifuge for 10 min at room temperature. The pellet was washed

with 500 µl of 70% cold ethanol and then dry under vacuum. The DNA pellet was dissolve in 50 µl of sterilized distilled water.

1.9 Restriction Analysis

Each mutant was screened by restriction analysis. The restriction enzyme recognition sites, silently introduced into the oligonucleotide primers, are *Sau*96I in pA182P, *Hpa*II in pL186P, *Hha*I in Y220P and pI221P, *Hinf*I in pT254P.and *Xba*I in pV257P. The 20 µl digestion reaction was composed of 0.5-1 µg of DNA sample, 1x restiction enzyme digestion buffer, and approximately 5 U of restriction endonuclease and sterilized distilled water to make up the 20 µl total volume. The digestion reaction was incubated at 37°C for 2 hours with appropriate enzymes. The recommended restriction enzyme digestion buffers were supplied by enzyme manufacturers. To visualize the restriction patterns, electrophoresis of the digested DNA was carried out in a horizontal 0.8% agarose gel in TB buffer at 100 V for an hour.

1.10 DNA Sequence Analysis

The DNA sequencing reactions were performed with ABI PRISM™ Dye Terminator Cycle Sequencing Ready Reaction Kit (Perkin Elmer) and performed on ABI PRISM™ 377 DNA Sequencer (Perkin Elmer) and using Q149PF as sequencing primer.

2. Expression and Purification of Toxins

2.1 Expression of Toxins

Each clone of the *E. coli* JM109 that carried the recombinant plasmid coding for the mutated toxin was picked from LB agar and grown in LB broth with 100 μg/ml ampicillin at 37°C and 250 rpm agitation. When the liquid culture reached 0.6-0.8 AU_{600}, IPTG was added to the final concentration of 0.2 mM and incubation continued at 37°C, 250 rpm for 4 hrs. Then, the culture was harvested by centrifugation at 3,000 rcf, 4°C for 10 min. The total *E. coli* protein was analysed on 10% SDS polyacrylamid gel.

2.2 Electrophoresis of Protein

2.2.1 Sample Preparation

Samples were mixed with 4x sample buffer [60 mM Tris-HCl (pH 7.5), 2%(w/v) SDS, 0.1% glycerol, 0.025%(w/v) Bromophenol blue, 100 mM DTT] in the ratio of 3:1, and boiled at 100°C for 5 min. The mixed samples were vigorously vortex mixed and centrifuged at 10,000 rpm for 10 min. When the sample was highly viscous $MgCl_2$ was added at the final concentration of 100 mM prior to boiling with 4x sample buffer (68).

2.2.2 SDS-PAGE

Electrophoresis of protein samples was performed by the method, described by Laemmli (69). SDS-PAGE was carried out using the Bio-Rad Mini-Protein II system. The separating gel contained 2.6%C, 10% or 12.5%T, 0.375 M Tris-HCl (pH 8.8), and

0.1% SDS. The stacking gel consisted of 2.6%C, 4%T, 0.125 M Tris-HCl (pH 6.8), and 0.1% SDS. The gel was run in Tris-glycine buffer (25 mM Tris, 192 mM glycine, and 0.1% SDS). Electrophoresis was performed with constant current of 20 mA per one gel of 0.75 mm thickness at room temperature.

After electrophoresis, the protein band on the gel was visualized by 1 hour soaking in staining solution containing 50% methanol, 10% glacial acetic acid and 0.1% Coomassie Brilliant Blue R-250 in water. The destaining was performed by soaking in destaining solution containing 10% methanol and 10% glacial acetic acid for 4 hours or until the background was clear.

2.3 Partial Purification of Inclusions

E. coli cells expressing the recombinant protein were harvested by centrifugation at 3,000 rcf. The harvested cells were resuspended in ice-cold distilled water at the ratio of 1 g cell (wet weight) per 2.5 ml water. The cell suspension was pressed through a French Pressure Cell at cell pressure 18,000 psi. The cell lysate was centrifuged at 8,000 rcf, 4°C for 15 min. The pellet was then washed twice in cold distilled water followed by sonication and centrifugation at 10,000 rpm, 4°C for 15 min. Both cell lysate and purified inclusions were analysed on 10% SDS polyacrylamide gel.

2.4 Protein Assays

Protein concentrations of partial-purified inclusions were determined by using Bio-Rad Protein microassay reagent and bovine serum albumin fraction V as

standards. The employed assay procedures are described in Bio-Rad Protein Assay Manual provided from Bio-Rad. To prepare the concentration standard protein samples, bovine serum albumin was diluted into 5 concentrations containing 2, 4, 6, 8 and 10 μg in 800 μl of distilled water. The sample solution in 800 μl was mixed with 200 μl of dye reagent. After 10 min. incubation at room temperature, the 595 nm absorbance of samples and standards were measured using Hitachi U-2000 spectrophotometer. The protein concentrations of samples were calculated from the standard curve.

3 Biochemical Characterization of Toxins

3.1 Solubilization of Toxins

One mg of each protoxin inclusion was centrifuged at 10,000 rpm for 10 min. The inclusion pellets were resuspended.in 1 ml of 50 mM Na_2CO_3, pH 9.0 and then incubated at 37°C for 1 hour. For solubility determination, the incubated toxins were subjected to centrifugation at 10,000 rpm for 10 min. Prior- and post-centrifugation toxin samples were quantitated as described in **METHOD 2.4**. Furthermore, the samples were mixed with loading buffer and then applied to 12.5% SDS polyacrylamide gel.

3.2 Protease Cleavage of Toxins

One mg of each protoxin inclusion was centrifuged at 10,000 rpm for 10 min. and then resuspended in 1 ml of 50 mM Na_2CO_3, pH 9.0, supplemented with trypsin (N-Tosyl-L-Phenylalanine Chloromethyl Ketone treated, Sigma) at a trypsin : protoxin

ratio of 1:20 (w/w). The suspension was incubated at 37°C for about 16 hours. To obtain soluble digested products, the incubated toxins were subjected to centrifugation at 10,000 rpm for 10 min. Both prior- and post-digested samples were mixed with loading buffer and then applied to 12.5% SDS polyacrylamide gel to determine the proteolytic susceptibility of the toxins.

4 *In vivo* Toxicity Assay

Mosquito bioassays were performed by using 2-day-old *Aedes aegypti* larvae, obtained from the mosquito-rearing facility of the Institute of Molecular Biology and Genetics, Mahidol university. Each recombinant *E. coli* sample was grown in LB broth with 100 μg/ml ampicillin. Protein expression was induced as described in **Method 2.1**. Cell pellet was harvested by centrifugation at 3,000 rcf for 15 min, resuspended in 1/10 of original volume distilled water and diluted to 5.0 AU_{600} ($5x10^8$ cells/ml). Each assay was performed in a 48-well titration plate (11.3 mm well diameter, Costar, MA, USA), containing 10 larvae in 800 μl of distilled water. Then, 200 μl of induced *E. coli* sample (10^8 cells) was added into each well. A total 100 larvae were used for each sample in one experiment. Two independent experiments were performed. The mortality was recorded and analyzed after 24-hour incubation at room temperature.

CHAPTER V

RESULTS

1. Construction of Cry4B Mutant Plasmids

Site-directed mutagenesis was performed in order to make single proline substitutions in the middle regions of selected helices of the 130 kDa Cry4B toxin, including Ala-182 and Leu-186 of helix 5, Tyr-220 and Ile-221 of helix 6 and Thr-254 and Val-257 of helix 7 (See **Fig. 7**). Five selected amino acid residues *i.e.* Ala-182, Leu-186, Tyr-220, Thr-254 and Val-257 are highly conserved in the delta-endotoxin family whereas Ile-221 and not. (See **Fig. 2**)

Each mutant plasmid was generated via PCR amplification using the recombinant plasmid pMU388 containing the gene sequence encoding the 130-kDa Cry4B toxin as a template. Each pair of mutagenesis primers was designed to introduce the a mutated nucleotide and a new restriction enzyme recognition sequence to identify PCR products by using an appropriate restriction enzyme.

The PCR conditions were optimized for the conditions to yield only one major product for each reaction (**Fig. 8-12**). The *Pfu* DNA polymerase containing proofreading activity was chosen to achieve high fidelity of the reaction. However, a high amount of PCR template and more PCR cycles (up to 25) were needed in order to increase the yield of product in certain PCR reactions. By employing high

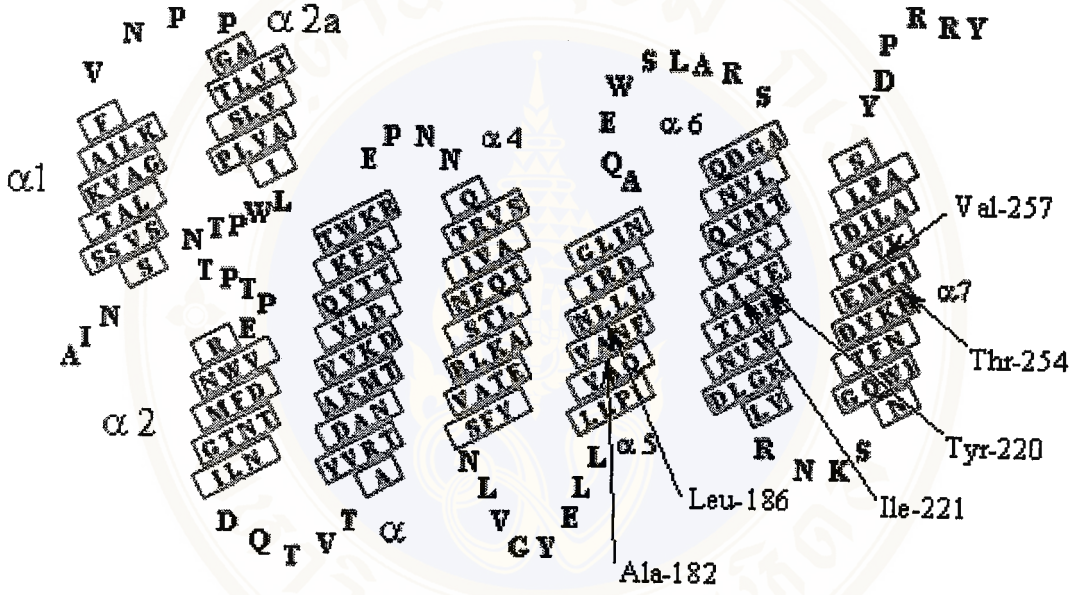

Figure 7 : Selected Residues for Proline Replacement in Cry4B

The figure shows the positions of six amino acid residues which are replaced with proline in three selected helices of the seven-helix bundle domain of the Cry4B toxin.

Figure 8 : Amplification of the mutant plasmid pL186P

The figure shows 0.8% agarose gel electrophoresis (ethidium bromide stained) of PCR product, using L186PF and L186PR as primers, pMU388 (100 ng) as PCR template and 45°C as annealing temperature.

Lane 1 : *Hin*dIII digested lambda DNA marker
Lane 2 : The PCR product of the tentative mutant plasmid pL186P

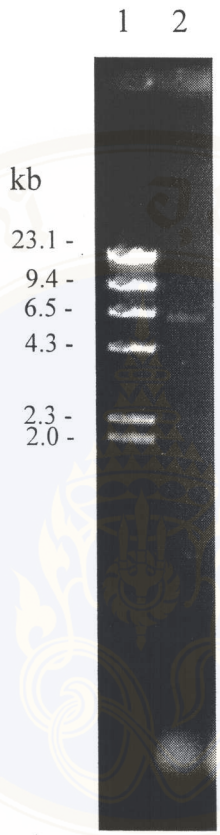

Figure 9 : Amplification of the mutant plasmid pY220P

The figure shows 0.8% agarose gel electrophoresis (ethidium bromide stained) of PCR product, using Y220PF and Y220PR as primers, pMU388 (100 ng) as PCR template and 40°C as annealing temperature

Lane 1 : *Hin*dIII digested lambda DNA marker
Lane 2 : The PCR product of the tentative mutant plasmid pY220P

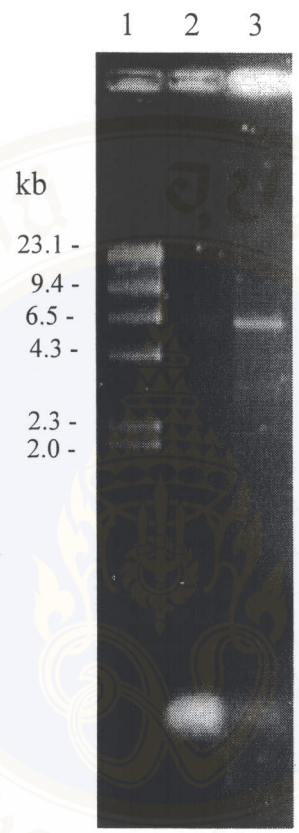

Figure 10 : Amplification of the mutant plasmid pT254P, using different amount of PCR template.

The figure shows 0.8% agarose gel electrophoresis (ethidium bromide stained) of PCR product, using T254PF and T254PR as primers, pMU388 as PCR template.and 45°C as annealing temperature

Lane 1 : *Hin*dIII digested lambda DNA marker
Lane 2 : The PCR product of the tentative mutant plasmid pT254P, using 100 ng of pMU388 as PCR template
Lane 3 : The PCR product of the tentative mutant plasmid pT254P, using 300 ng of pMU388 as PCR template

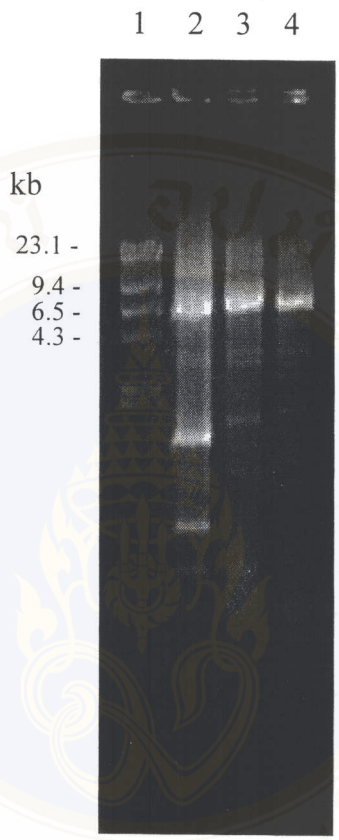

Figure 11 : Amplification of the mutant plasmid pA182P, using different annealing temperature

The figure shows 0.8% agarose gel electrophoresis (ethidium bromide stained) of PCR product, using A182PF and A182PR as primers and PCR (300 ng) template.

Lane 1 : *Hin*dIII digested lambda DNA marker
Lane 2 : The PCR product of the tentative mutant plasmid pA182P, using 45 °C as annealing temperature.
Lane 3 : The PCR product of the tentative mutant plasmid pA182P, using 48 °C as annealing temperature.
Lane 4 : The PCR product of the tentative mutant plasmid pA182P, using 50 °C as annealing temperature.

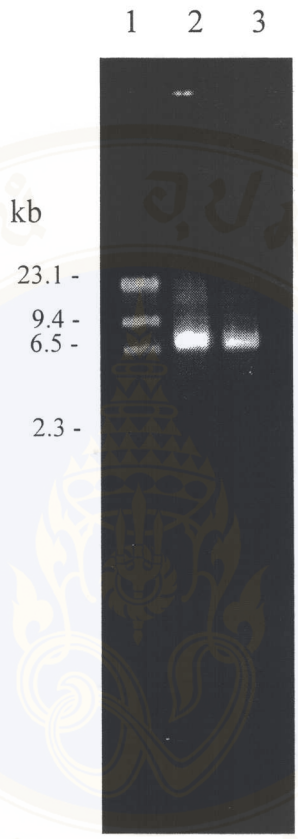

Figure 12 : Amplification of the mutant plasmid pI221P and pV257P

The figure shows 0.8% agarose gel electrophoresis (ethidium bromide stained) of two different PCR products, pI221P and pV257P which were obtained by using 300 ng of pMU388 as PCR template and 48°C as annealing temperature

Lane 1 : *Hin*dIII digested lambda DNA marker
Lane 2 : The PCR product of the tentative mutant plasmid pI221P
Lane 3 : The PCR product of the tentative mutant plasmid pV257P

amount of PCR template as described in **Fig. 10**, the large amount of the pT254P PCR product was achieved, but there were a number of nonspecific products.

As annealing temperature could also be another factor that would affect the specificity of PCR product, the highest annealing temperature that could generate the optimal PCR product was chosen. As can be seen in **Fig. 11 (lane 4)** at annealing temperature of 50°C, the PCR product obtained for the pA182P mutant plasmid was specific and the yield was considerably high.

After digesting the methylated and hemimethylated plasmid DNA with *Dpn*I (target sequence 5′-G_{m6}ATC-3′), the digested PCR products were transformed into *E. coli* JM109. About 50 transformants were obtained for each mutant. Ten transformants of each mutant were picked for restriction analysis. The plasmid from each colony was extracted and cut with an appropriate restriction enzyme and the predicted restriction patterns for each mutant were shown in **Table 1**. And the examples of them were shown in **Fig. 13-18**. It was found that at least two to three mutant plasmid clones were obtained for each mutation.

The plasmid of of Ala-182 mutants can be distinguished from the wild type plasmid, pMU388, by inspecting the *Sau96*I digested products for ca 2.4-kb band of the wild type plasmid (**Fig. 13, lane 2**) and the ca 2.0-kb band of the mutant plasmid (**Fig 13, lane 3**). The plasmid of Leu-186 mutants could be distinguished from the wild type by inspecting the *Hpa*II digested products for ca 1.6-kb band of the wild type plasmid (**Fig. 14, lane 1**) and the ca 0.9- and 0.7-kb bands of the mutant plasmid (**Fig. 14, lane 2**). Also, the plasmids of Tyr-220 or Ile-221 mutants were be able to be distinguished from the wild type plasmid by inspecting the *Hha*I digested products for

Table 1 : Predicted patterns for restriction analysis of mutant plasmids

Table shows the restriction enzymes and DNA fragments which could be used in restriction analysis of mutant plasmids.

Plasmid	Restriction Enzyme	Wild-type plasmid fragment (kb)	Mutant plasmid fragment (kb)
pA182P	*Sau*96I	2.4	2.0 + 0.4
pL186P	*Hpa*II	1.6	0.9 + 0.7
pY220P	*Hha*I	2.8	2.4 + 0.4
pI221P	*Hha*I	2.8	2.4 + .04
pT254P	*Hin*fI	0.6	ND
pV257P	*Xba*I	ND	0.9

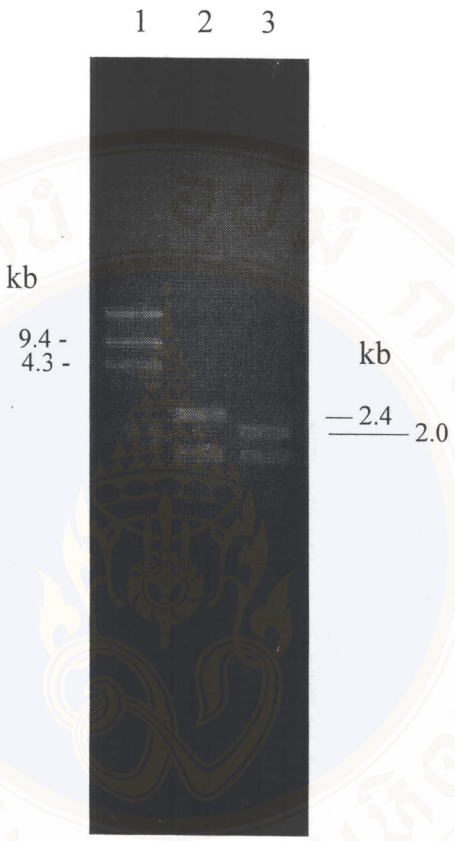

Figure 13 : Restriction endonuclease analysis of pA182P mutant plasmid

The figure shows 0.8% agarose gel electrophoresis (ethidium bromide stained) of *Sau*96I digestion patterns of mutant plasmid in comparison with that of wild type plasmid.

Lane 1 : *Hin*dIII digested lambda DNA marker
Lane 2 : pMU388 digested with *Sau*96I
Lane 3 : pA182P digested with *Sau*96I

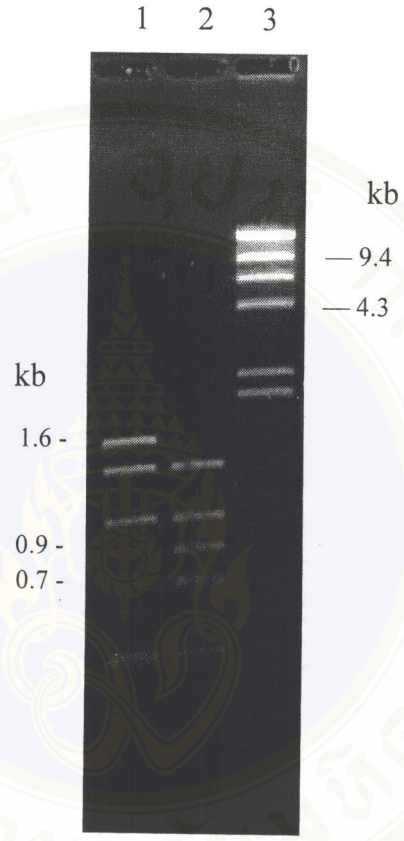

Figure 14 : Restriction endonuclease analysis of pL186P mutant plasmid

The figure shows 0.8% agarose gel electrophoresis (ethidium bromide stained) of *Hpa*II digestion patterns of mutant plasmid in comparison with that of wild type plasmid.

Lane 1 : pMU388 digested with *Hpa*II
Lane 2 : pL186P digested with *Hpa*II
Lane 3 : *Hin*dIII digested lambda DNA marker

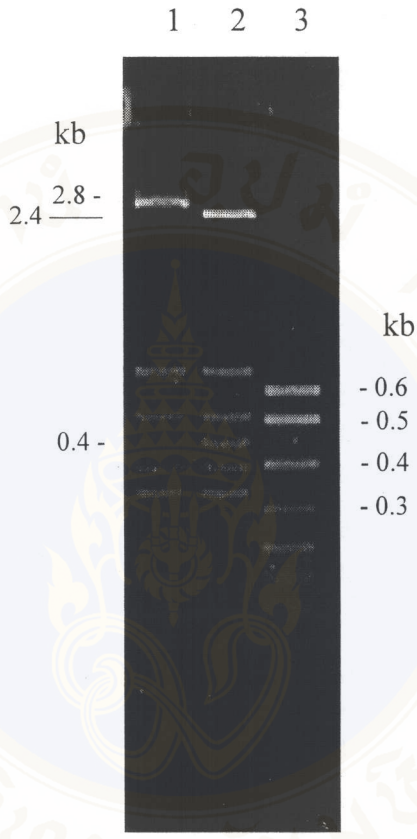

Figure 15 : Restriction endonuclease analysis of pY220P mutant plasmid

The figure shows 1.0% agarose gel electrophoresis (ethidium bromide stained) of *Hha*I digestion patterns of mutant plasmid in comparison with that of wild type plasmid.

Lane 1 : pMU388 digested with *Hha*I
Lane 2 : pY220P digested with *Hha*I
Lane 3 : *Msp*I digested pBR322 DNA marker

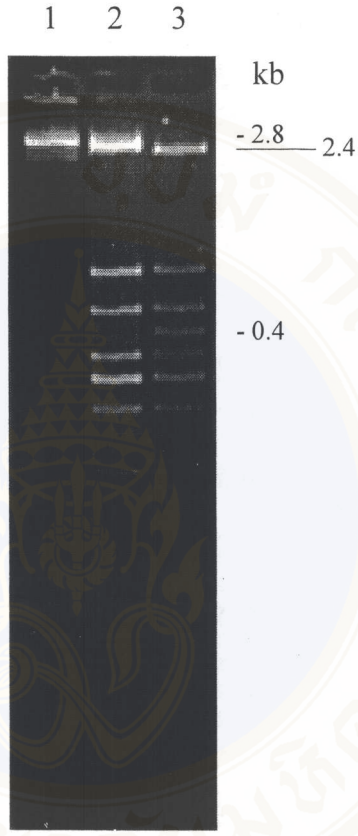

Figure 16 : Restriction endonuclease analysis of pI221P mutant plasmid

The figure shows 1.2% agarose gel electrophoresis (ethidium bromide stained) of *Hha*I digestion patterns of mutant plasmid in comparison with that of wild type plasmid.

Lane 1 : *Hin*dIII digested lambda DNA marker
Lane 2 : pMU388 digested with *Hha*II
Lane 3 : pI221P digested with *Hha*II

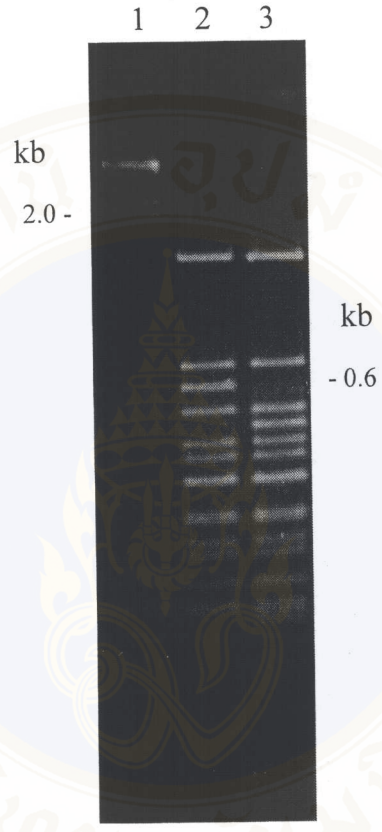

Figure 17 : Restriction endonuclease analysis of pT254P mutant plasmid

The figure shows 1.0% agarose gel electrophoresis (ethidium bromide stained) of *Hin*fI digestion patterns of mutant plasmid in comparison with that of wild type plasmid.

Lane 1 : *Hin*dIII digested lambda DNA marker
Lane 2 : pMU388 digested with *Hin*fI
Lane 3 : pT254P digested with *Hin*fI

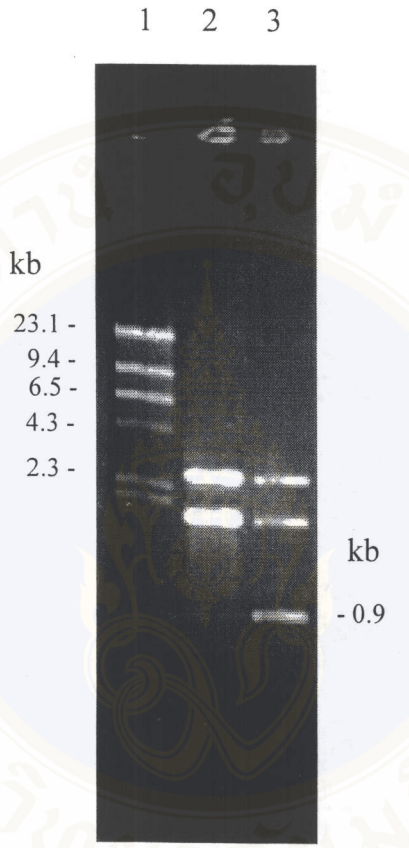

Figure 18 : Restriction endonuclease analysis of pV257P mutant plasmid

The figure shows 0.8% agarose gel electrophoresis (ethidium bromide stained) of *Xba*I digestion patterns of mutant plasmid in comparison with that of wild type plasmid.

Lane 1 : *Hin*dIII digested lambda DNA marker
Lane 2 : pMU388 digested with *Xba*II
Lane 3 : pV257P digested with *Xba*II

ca 2.8-kb band of the wild type plasmid (**Fig 15, lane 1; Fig 16, lane 2**) and the ca 2.4- and 0.4-kb bands of both mutant plasmids (**Fig. 15, lane 2; Fig. 16, lane 3**). Similarly, the plasmid of Thr-254 mutants could be distinguished from the wild type by inspecting the *Hin*fI digested products for ca 0.6 kb-band of the wild type plasmid (**Fig. 17, lane 2**) and for disappearing of the 0.6-kb band of the mutant plasmid (**Fig 17, lane 3**). By the similar way, the plasmid of Val-257 mutants was distinguished from the wild type pMU388 by inspecting the *Xba*I digested products for ca 0.9-kb band of the mutant plasmids (**Fig. 18, lane 3**).

After the mutant plasmid were expressed in *E. coli* cells and analyzed on SDS-PAGE, only mutant plasmids that yielded 130-kDa protoxin in the comparable levels to wild type, were analyzed by DNA sequencing. As shown in **Appendix 3**, the verified sequences do not accommodate any undesired mutation located in the sequenced regions.

2. Expression of the Mutant Toxins

All restriction analyzed mutants were cultured in LB broth and induced with IPTG as described in **CHAPTER IV**. The crude extracts, the supernatant and the sedimented protein fractions were analyzed on SDS-PAGE. It was found that some mutant clones expressed the 130-kDa protein at very low levels. Clones displaying highest level of expression were picked for further analysis.

Similar to the wild-type Cry4B toxin, the chosen mutant toxins were over-expressed as cytoplasmic inclusions by IPTG induction for 4 hours. It was found that expression levels of some induced mutants were lower than that of the wild type. The problem could be overcome by extending the induction duration from 4 hours to 6 hours. As can be seen in **Fig. 19**, the protein expression levels of the A182P, L186P, Y220P, I221P, T254P and V257P mutants are apparently the same as for the wild type.

3. Partial Purification of Mutant Toxin Inclusions

All mutant toxin cytoplasmic inclusions were partially purified as described in **CHAPTER IV**. Protein concentrations of partially purified inclusions were determined by using Bio-Rad Protein microassay reagent and bovine serum albumin fraction V as a standard. IPTG induced *E. coli* cells containing pMU388, pA182P, pL186P, pY220P, pI221P, pT254P and pV257P yielded the purified inclusions at 19, 18, 17, 16, 21, 17 and 19 μg/ml of 1 AU_{600} cell suspensions, respectively.

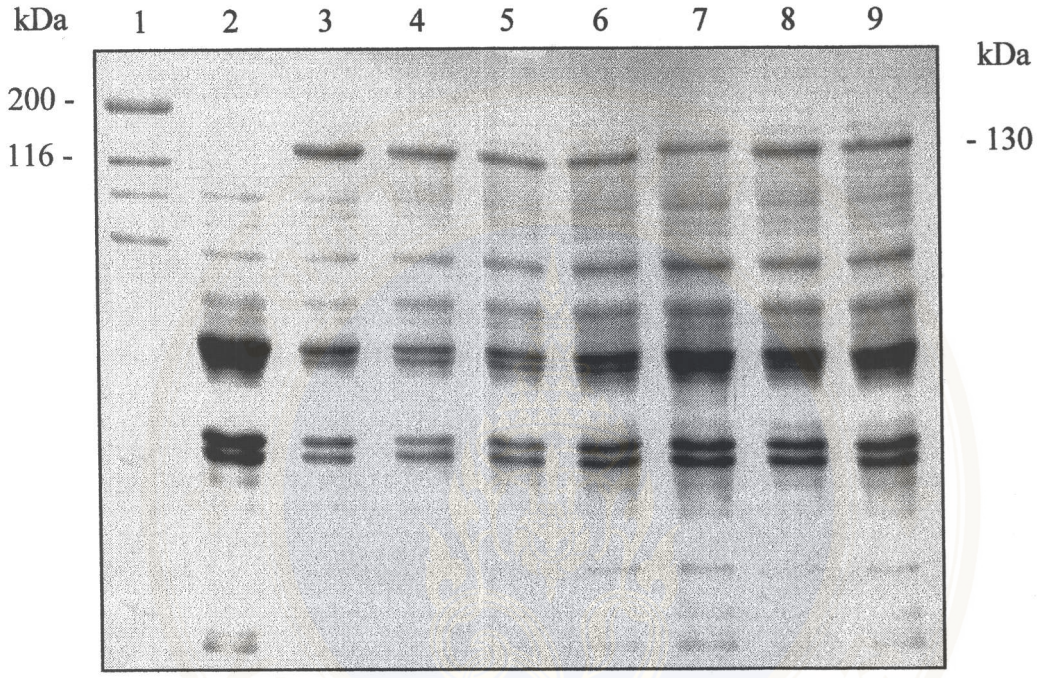

Figure 19 : Expression level of the Cry4B toxin and its mutants

The figure shows SDS-PAGE (Coomassie blue stained 10% gel) of the crude extracts of 6-hour IPTG induced recombinant *E. coli* cells containing different plasmids.

Lane 1 : molecular mass protein standards
Lane 2 : crude extracted protein of *E. coli* containing pUC12
Lane 3 : crude extracted protein of *E. coli* containing pMU388
Lane 4 : crude extracted protein of *E. coli* containing pA182P
Lane 5 : crude extracted protein of *E. coli* containing pL186P
Lane 6 : crude extracted protein of *E. coli* containing pY220P
Lane 7 : crude extracted protein of *E. coli* containing pI221P
Lane 8 : crude extracted protein of *E. coli* containing pT254P
Lane 9 : crude extracted protein of *E. coli* containing pV257P

4. Biochemical Characterization of Mutant Toxins

4.1 Solubility of Mutant Toxins

The partially purified inclusions of each mutant toxin were subjected to 1 hour solubilization in carbonate buffer pH 9.0, in comparison with the wild type inclusions which exhibit more than 50% solubility. When the mutant toxin inclusions were accessed for their solubility, it was found that all six mutant inclusions could hardly dissolve in this buffer (**Fig. 20-21** and **Table 2**). Although an incubation time was extended to 24 hours it still yielded aggregated insoluble products.

Table 2 : Solubility of Cry4B and its mutant toxins

The table shows solubility of the Cry4B and its mutant inclusions. The toxins were incubated for 1 hr with carbonate buffer (pH 9.0) and centrifuged at 10,000 for 10 min. 5 µl of Prior- and post-centrifugation toxin samples were subjected to protein quantitative assay as described in **METHOD 2.4**

Toxin	% Solubility
Cry4B (wild type)	61
A182P	1.2
L186P	0.42
Y200P	0.24
I221P	0.25
T254P	0.02
V257P	0.32

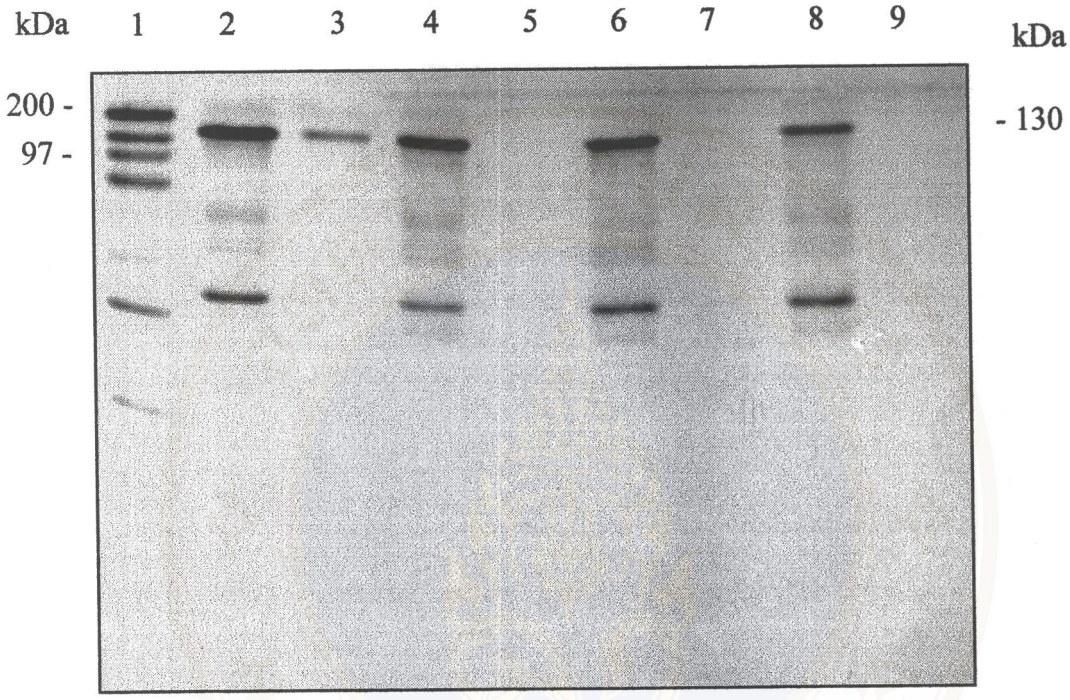

Figure 20 : Solubility of the Cry4B toxin inclusion and its mutant inclusions

The figure shows SDS-PAGE (Coomassie blue stained 12.5% gel) of the Cry4B and its mutant inclusions. The toxins were incubated for 1 hr with carbonate buffer (pH 9.0) and centrifuged at 10,000 for 10 min. 3 µl of Prior- and post-centrifugation toxin samples were mixed with loading buffer and then applied to the gel.

Lane 1 : molecular mass protein standards
Lane 2 : the partially purified wild-type Cry4B inclusion
Lane 3 : the solubilized wild-type Cry4B toxin
Lane 4 : the partially purified A182P mutant protein inclusion
Lane 5 : the solubilized A182P mutant protein
Lane 6 : the partially purified L186P mutant protein inclusion
Lane 7 : the solubilized L186P mutant protein
Lane 8 : the partially purified Y220P mutant protein inclusion
Lane 9 : the solubilized Y220P mutant protein

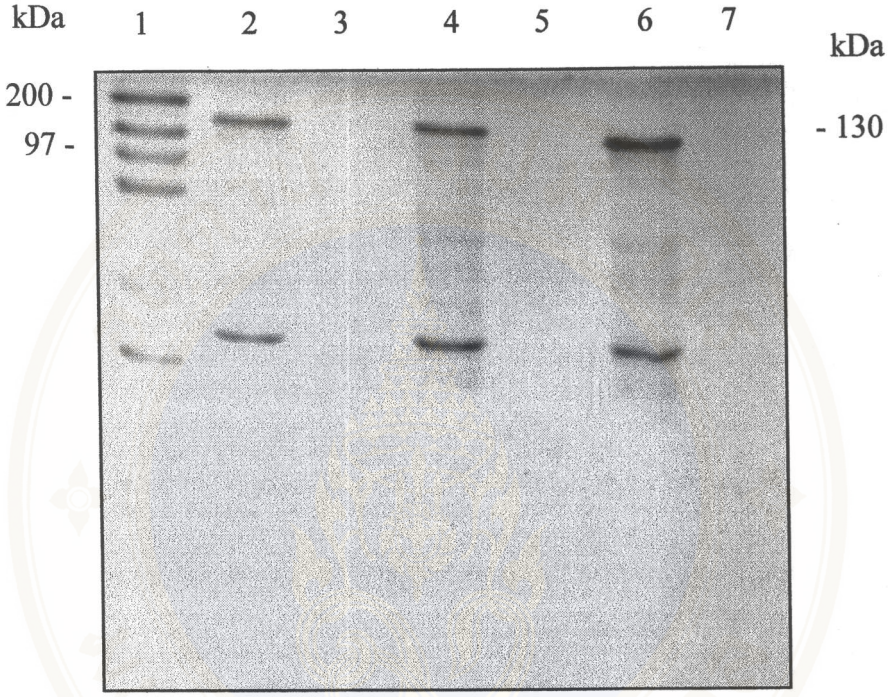

Figure 21 : Solubility of the mutant Cry4B toxin inclusions

The figure shows SDS-PAGE (Coomassie blue stained 12.5% gel) of the Cry4B mutant inclusions. The toxins were incubated for 1 hr with carbonate buffer (pH 9.0) and centrifuged at 10,000 for 10 min. 3 µl of Prior- and post-centrifugation toxin samples were mixed with loading buffer and then applied to the gel.

Lane 1 : molecular mass protein standards
Lane 2 : the partially purified I221P mutant protein inclusion
Lane 3 : the solubilized I221P mutant protein
Lane 4 : the partially purified T254P mutant protein inclusion
Lane 5 : the solubilized T254P mutant protein
Lane 6 : the partially purified V257 mutant protein inclusion
Lane 7 : the solubilized V257P mutant protein

4.2 Proteolytic Cleavage of Mutant Toxins

An attempt was made to solubilise the mutant inclusions in the presence of trypsin. Similar to the wild-type Cry4B toxin, upon treatment with trypsin, the mutant toxins would give trypsin resistant degradation products of ca. 47 and 18 kDa. Purified inclusions were subjected to solubilization in the carbonate buffer pH 9.0 supplemented with 1:20 (w/w) trypsin:toxin. After 16-hr incubation at 37°C, the proteolytic products were analyzed on SDS-polyacrylamide gel as shown in (**Fig. 22-24**). None of the mutant inclusions produced the soluble trypsin resistant products (ca. 47 and 18 kDa). The mutant protoxin inclusions were apparently digested to small soluble fragments, suggesting that the mutant protoxins may fold incorrectly leading to proteolytic degradation.

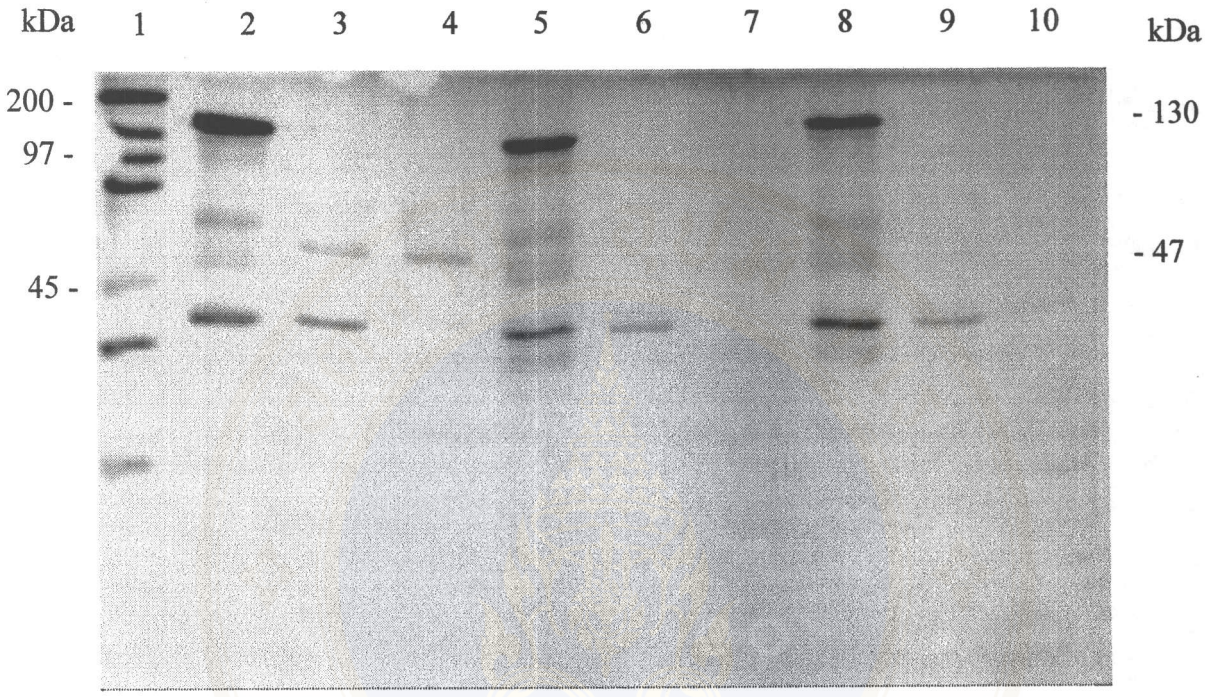

Figure 22 : Trypsinized products of Cry4B toxin and its mutants

The figure shows SDS-PAGE (Coomassie blue stained 12.5% gel) of the trypsinized products of Cry4B and its mutant inclusions. The toxins were incubated for 1 hr with carbonate buffer (pH 9.0) supplemented with trypsin and centrifuged at 10,000 for 10 min. 3 µl of Prior- and post-centrifugation toxin samples were mixed with loading buffer and then applied to the gel.

Lane 1 : molecular mass protein standards
Lane 2 : the partially purified wild-type Cry4B inclusion
Lane 3 : the total trypsinized product of Cry4B
Lane 4 : the soluble part of trypsinized products of the wild-type Cry4B toxin
Lane 5 : the partially purified A182P mutant inclusion
Lane 6 : the total trypsinized product of A182P mutant
Lane 7 : the soluble part of trypsinized product of A182P mutant
Lane 8 : the partially purified L186P mutant inclusion
Lane 9 : the total trypsinized product of L186P mutant
Lane 10 : the soluble part of trypsinized product of L186P mutant

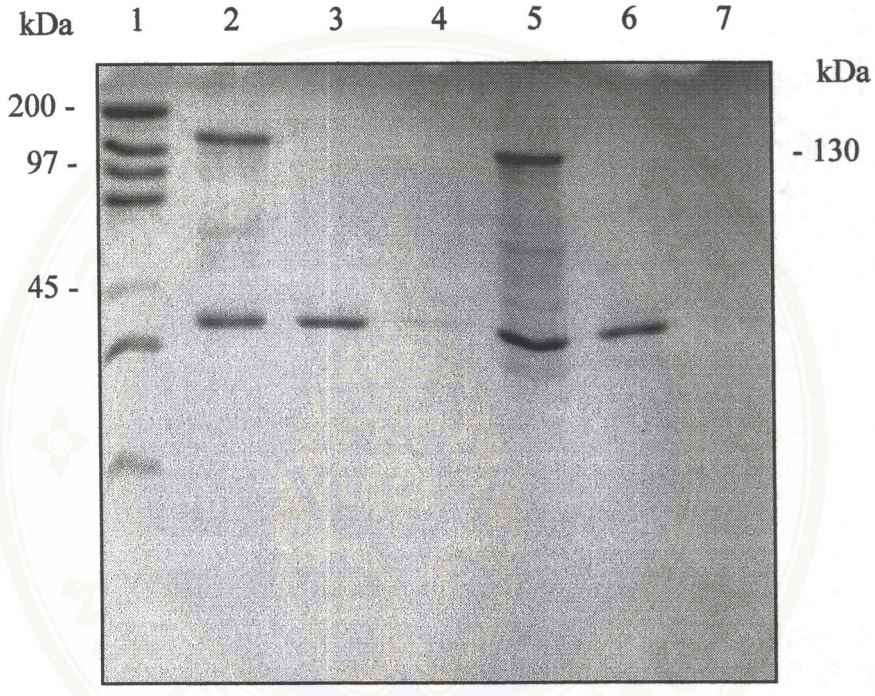

Figure 23 : Trypsinized products of mutant Cry4B toxins

The figure shows SDS-PAGE (Coomassie blue stained 12.5% gel) of the trypsinized products of Cry4B mutant inclusions. The toxins were incubated for 1 hr with carbonate buffer (pH 9.0) supplemented with trypsin and centrifuged at 10,000 for 10 min. 3 µl of Prior- and post-centrifugation toxin samples were mixed with loading buffer and then applied to the gel.

Lane 1 : molecular mass protein standards
Lane 2 : the partially purified Y220P mutant inclusion
Lane 3 : the total trypsinized product of Y220P mutant
Lane 4 : the soluble part of trypsinized product of Y220P mutant
Lane 5 : the partially purified I221P mutant inclusion
Lane 6 : the total trypsinized product of I221P mutant
Lane 7 : the soluble part of trypsinized product of I221P mutant

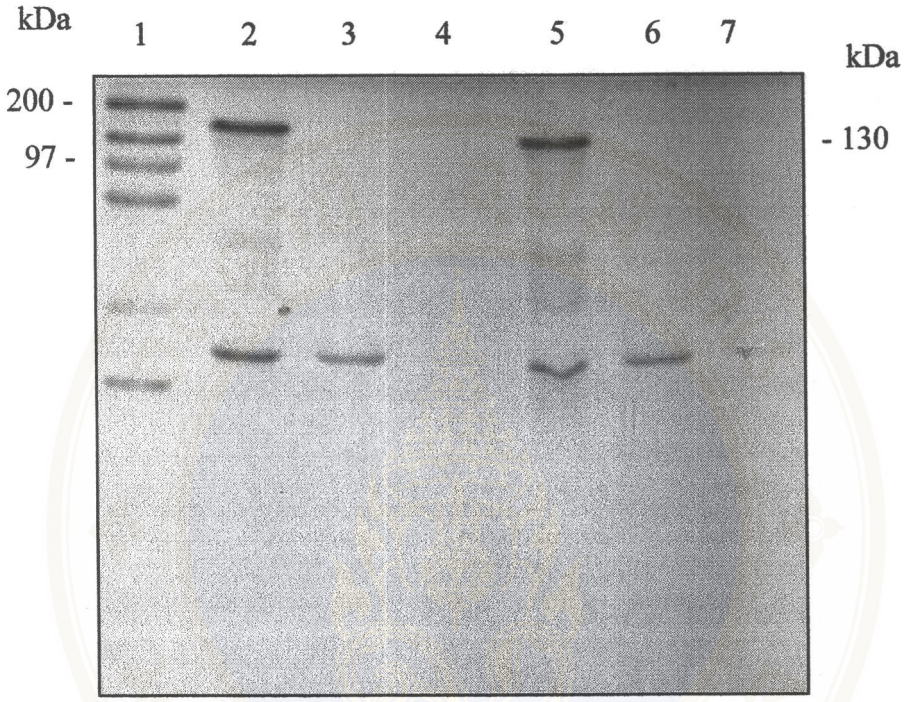

Figure 24 : Trypsinized products of mutant Cry4B toxins

The figure shows SDS-PAGE (Coomassie blue stained 12.5% gel) of the trypsinized products of Cry4B mutant inclusions. The toxins were incubated for 1 hr with carbonate buffer (pH 9.0) supplemented with trypsin and centrifuged at 10,000 for 10 min. 3 µl of Prior- and post-centrifugation toxin samples were mixed with loading buffer and then applied to the gel.

Lane 1 : molecular mass protein standards
Lane 2 : the partially purified T254P mutant inclusion
Lane 3 : the total trypsinized product of T254P mutant
Lane 4 : the soluble part of trypsinized product of T254P mutant
Lane 5 : the partially purified V257P mutant inclusion
Lane 6 : the total trypsinized product of V257P mutant
Lane 7 : the soluble part of trypsinized product of V257P mutant

5. Functional Characterization of Mutant

Bioassay experiments were performed by using *Aedes aegypti* larvae in order to assess larvicidal activity of these mutant toxin samples. *E. coli* cells containing either pUC12 vector, pMU388, pA182P, pL186P, pY220P, pI221P, pT254P or pV257P plasmids were induced with IPTG as the conditions described in **METHOD 2.1** and were used in the assays as described in **METHOD 4**. For two independent experiments using 100 larvae for each toxin sample, it was found that the mortality given by the wild-type toxin containing *E. coli* cells was 75.5%±10.5. However, the *E. coli* cells expressing either A182P, L186P, Y220P, I221P, T254P or V257P mutant toxin were not toxic to the larvae, as similar to negative control cells containing vector alone (see **Table 3**). The lost of toxicity might be due to low solubility of the mutant toxins as demonstrated in **RESULT 4.1** or distortion of the helices involved in toxicity.

Table 3 : Larvicidal activity of the *E. coli* clones containing mutant plasmids

The table shows larvicidal activities of Cry4B and its mutant toxins. The larvicidal activities were detected from the amount of living larvae after 24 hrs incubation with toxin expression *E. coli* cells. The data represent the mean±SEM, which are based on two separated assays.

E. coli containing plasmids	%Larvicidal Activity±SEM[a]
pUC12	3.0±3.7
Cry4B	75.5±10.5
A182P	2.0±4.1
L186P	2.0±2.6
Y220P	3.0±2.8
I221P	0.5±1.1
T254P	0.5±1.1
V257P	3.5±4.0

[a] SEM= $\frac{SD}{\sqrt{N}}$; [N = Sample size (2)]

CHAPTER VI

DISCUSSION

Our understanding of how the *Bt* insecticidal proteins function at the molecular level has increased substantially over the last decade, but several key questions still remain about their mechanism of action. Recently, structural data of two different Cry toxins, the coleopteran-specific Cry3A toxin (10) and the lepidopteran-specific Cry1A toxin (9) have been obtained by X-ray crystallography. They have shown that both toxins possess a similar organization of three-domain tertiary structure. The amino acid sequences encoded in domain I are highly conserved in the Cry toxin family.This bundle consisting of long, amphipathic helices is identified as a pore forming apparatus. Since only α3, α4, α5, α6 and α7 are long enough to be trans-membrane helices and this helical bundle is proposed as a pore-forming domain (9, 10) it would be expected a reduction of toxicity for the mutants that have a proline substitution on the trans-membrane responsive helix. This proposal was supported by the introduction a proline into α4 at the amino acid position 149 that almost completely eliminated the toxicity of Cry4B against *Aedes aegypti* mosquito-larvae (60).

Several studies were performed on α5 (12, 45, 46, 47, 62, 63, 64, 65) but only a few on α3 (59, 60), α4 (60), α6 or α7 (12, 63, 65). In this study, six proline substituted mutant proteins were designed based on a homology-based 3D model of the Cry4B toxin which was previously constructed by using Cry3A as a template (60). The designed Cry4B mutants have a single proline substitution in the central region of

selected helices including helix 5 at residues alanine-182 and leucine-186, helix 6 at residues tyrosine-220 and isoleucine-221 and helix 7 at residues threonine-254 and valine-257 in the domain I.

For solubility analysis, prior- and post-solubilized toxins were visualized on SDS-polyacrylamide gels. Unlike the wild-type Cry4B toxin which gave more than 50% solubility in alkaline environment (carbonate buffer pH 9.0), the A182P, L186P, Y220P, I221P, T254P and V257P mutant protoxin inclusions gave no soluble product that is detectable on Coomassie blue stained polyacrylamide gels. These indicate that the expressed mutant proteins may have an incorrect overall structure. Since all six mutated residues are amino acids that buried inside the molecule, proline substitution may disturb the local helix structure and then would affect overall structure of the toxin.

When the solubilized wild type Cry4B toxin was treated with trypsin *in vitro*, the proteolytic products contained two major polypeptides of ca. 47- and 18- kDa (60, 70, 71). In this study, the expressed Cry4B inclusion treated with trypsin while being solubilised in carbonate buffer also yielded two of major products, of ca. 47 kDa and 18 kDa on SDS-polyacrylamide gel but the trypsin digested products of the mutant Cry4B inclusions yielded no trypsin resistant product on the gel. This difference could be that the mutant protoxins formed in the inclusions might not adopt the same conformation as that in the native Cry4B inclusion. The mutant conformation might allow other trypsin cleavage sites located in the molecule being more exposed to protease attack.

Results from bioassays (**Table 1**) were consistent with biochemical properties. The fact that all the mutant proteins were not toxic to mosquito larvae did not exhibit

the same solubility as the wild type and gave no stable tryptic digestion products. Therefore the effect on larvicidal activity seen for these mutants are likely to be due to misfolding which leads to structural instability.

Bosch et al. (72) have demonstrated the relation of biological activity and biochemical properties of the engineered Cry toxin. In contrast to the wild-type, expression of the mutant alleles in *E. coli* resulted in the formation of biologically inactive, insoluble aggregates. Although these aggregates could be solubilized *in vitro* using urea, the solubilized proteins could not be correctly refolded being shown by their increasing protease sensitivity and lack of biological activity. Another site-directed mutagenesis experiment on Cry1Ab also suggested that the proteolytic processing could be used in examining for structural differences between native and mutant proteins (73).

There is no evidence showing that the seven-helix bundle domain is involved in the protoxin folding. However Ort et al. (74) have performed an experiment on denaturation of Cry3A and suggested that the domain I part would play a less important role in the protein folding.

The results of this study imply that the proline replacements in the three non-solvent exposed helices could have a direct effect on protein solubility, protease susceptibility and toxicity of Cry4B toxin (see **Table 4**). Proline substitution in the middle region of an alpha helix might not be the most appropriate approach for trans-membrane helix scanning in α5, α6 and α7 of Cry4B toxin. The incomparable biochemical properties of the mutant toxin are obstacles in trans-membrane investigation. It also is implied that the structure of such helices may play an important role in native folding of the toxin.

Table 4 : Biochemical and biological properties of Cry4B toxin and its mutants.
The inclusions of expressed protoxins were solubilized in carbonate buffer pH 9.0, exposed to proteolytic processing and subjected to larvicidal activity assay.

Protein	Solubility	Proteolytic digestion	%Larvicidal Activity±SEM[b]
Cry4B	+[a]	+	75.5±10.5
A182P	-	-	2.0±4.1
L186P	-	-	2.0±2.6
Y220P	-	-	3.0±2.8
I221P	-	-	0.5±1.1
T254P	-	-	0.5±1.1
V257P	-	-	3.5±4.0

[a] - The + symbol represents positive result for the experiments which showed (1) over 50% of soluble product within 1 hr (2) ca 47- and 18-kDa soluble products on SDS-acrylamide gel.
[b] SEM= $\frac{SD}{\sqrt{N}}$; [N = Sample size (2)]

Three explanations could be made. Firstly, the kink part of the selected helix would interfere with helix bundle formation in domain I, and thus deform the whole molecule. Second, unfavorably exposed regions produced by a new intrahelical hydrogen network, C--H...O, might dissatisfy the hydrophobic surrounding of selected residues. Third, it is likely to form a water-filled pocket caused by a kink in the helix located at the domain interface that would be expected to impair proper organization among domain I, II and III. The structurally important salt bridges are conserved across Cry sequences and their possible role in toxin action was postulated (9). Disruption of the interdomain alpha-helices i.e. α6 and α7 by at least two unsatisfied hydrogen bonds and a newly formed water-filled protruding into the hydrophobic core, could possibly reduce the stabilizing contribution of a partially buried interdomain salt bridge. It was also found that mutations in the salt bridge formed by Asp-242 and Arg-265 i.e. D242N, D242C, R265C, and D242C/R265C of Cry1Ab resulted in structurally unstable mutant proteins as being shown by their increased protease

sensitivity and lack of biological activity (72). These indicating that the proline replacements of some amino acids in α5, α6 and α7 mutant toxin would disturb overall structure of the toxins and yield structural unstable delta-endotoxin inclusions.

CHAPTER VII

CONCLUSION

1. Six Cry4B mutant toxin coding plasmids which have proline substitution in the middle region of α5 that are pA182P and pL186P, α6 that are pY220P and pI221P, α7 that are pT254P and pV257P were constructed via site-directed mutagenesis based in PCR technique and using pMU388 as the PCR template. The sequences of mutant plasmids were confirmed by automated DNA sequencing and found that there is no other undesired mutation in the sequenced regions.

2. The PCR products were transformed into *E. coli* strain JM109. The mutant plasmid clones were analyzed by using restriction enzymes. The mutant plasmids were expressed in the *E.coli* strain JM 109 as cytoplasmic inclusions at wild-type levels.

3. The expressed protoxin were purified in the form of insoluble inclusion. The solubility of all protoxin inclusions were examined by incubation for 1 hr at 37°C in carbonate buffer, pH 9.0. The wild type inclusion yielded the 130-kDa soluble product while the mutant protoxin inclusions were found to be insoluble.

4. When the protoxin inclusions were incubated in carbonate buffer supplemented with trypsin for 12 hrs, the wild type Cry4B protoxin was clearly processed to ca.

47- and 18-kDa soluble products while the mutant protoxins were digested to small soluble fragments which were not detected on SDS-PAGE.

5. The *E. coli* containing mutant plasmids, pA182P, pL186P, pY220P, pI221P, pT254P or pV257P was less toxic to *Aedes aegypti* larvae. Changes in toxicity of these six mutant clones were in agreement with changes in the solubility and proteolytic endurance of the mutant protoxin inclusions.

REFERENCES

1. Knowles BH. Mechanism of action of *Bacillus thuringiensis* insecticidal δ-endotoxin. Adv Insect Physiol 1994;24:276-307
2. Hofte H, Whiteley HR. Insecticidal crystal proteins of *Bacillus thuringiensis*. Microbiol Rev 1989;53(2):242-55
3. Aronson AI, Beckman W, Dunn P. *Bacillus thuringiensis* and related insect pathogens. Microbiol Rev 1986;50(1):1-24
4. Prieto-Samsonov DL, Vazquez-Padron RI, Ayra-Pardo C, Gonzalez-Cabrera J, de la Riva GA. *Bacillus thuringiensis*: from biodiversity to biotechnology. J Ind Microbiol Biotechnol 1997;19(3):202-19
5. Crickmore N, Zeigler DR, Feitelson J, Schnepf E, Van Rie J, Lereclus D, Baum J, Dean DH. Revision of the nomenclature for the *Bacillus thuringiensis* pesticidal crystal proteins. Microbiol Mol Biol Rev 1998;62(3):807-13
6. Angsuthanasombat C, Chungjatupornchai W, Kertbundit S, Luxananil P, Settasatian C, Wilairat P, Panyim S. Cloning and expression of 130-kd mosquito-larvicidal delta-endotoxin gene of *Bacillus thuringiensis* var. *Israelensis* in *Escherichia coli*. Mol Gen Genet 1987 Jul;208(3):384-9
7. Chungjatupornchai W, Hofte H, Seurinck J, Angsuthanasombat C, Vaeck M. Common features of *Bacillus thuringiensis* toxins specific for Diptera and Lepidoptera. Eur J Biochem 1988;173(1):9-16

8. Kumar PA, Sharma RP, Malik VS. The insecticidal proteins of *Bacillus thuringiensis*. Adv Appl Microbiol 1996;42:1-43

9. Grochulski P, Masson L, Borisova S, Pusztai-Carey M, Schwartz JL, Brousseau R, Cygler M. *Bacillus thuringiensis* CryIA(a) insecticidal toxin: crystal structure and channel formation. J Mol Biol 1995;254(3):447-64

10. Li JD, Carroll J, Ellar DJ. Crystal structure of insecticidal delta-endotoxin from *Bacillus thuringiensis* at 2.5 A resolution. Nature 1991;353(6347):815-21

11. Schwartz JL, Juteau M, Grochulski P, Cygler M, Prefontaine G, Brousseau R, Masson L. Restriction of intramolecular movements within the Cry1Aa toxin molecule of *Bacillus thuringiensis* through disulfide bond engineering. FEBS Lett 1997;410(2-3):397-402

12. Gazit E, La Rocca P, Sansom MS, Shai Y. The structure and organization within the membrane of the helices composing the pore-forming domain of *Bacillus thuringiensis* delta-endotoxin are consistent with an "umbrella-like" structure of the pore. Proc Natl Acad Sci U S A 1998;95(21):12289-94

13. Dean DH, Rajamohan F, Lee MK, Wu SJ, Chen XJ, Alcantara E, Hussain SR. Probing the mechanism of action of *Bacillus thuringiensis* insecticidal proteins by site-directed mutagenesis. Gene 1996;179(1):111-7

14. Chen XJ, Curtiss A, Alcantara E, Dean DH. Mutations in domain I of *Bacillus thuringiensis* delta-endotoxin CryIAb reduce the irreversible binding of toxin to *Manduca sexta* brush border membrane vesicles. J Biol Chem 1995;270(11):6412-9

15. Von Tersch MA, Slatin SL, Kulesza CA, English LH. Membrane-permeabilizing activities of *Bacillus thuringiensis* coleopteran-active toxin CryIIIB2 and CryIIIB2 domain I peptide. Appl Environ Microbiol 1994;60(10):3711-7

16. Ge AZ, Rivers D, Milne R, Dean DH. Functional domains of *Bacillus thuringiensis* insecticidal crystal proteins. Refinement of *Heliothis virescens* and *Trichoplusia ni* specificity domains on CryIA(c). J Biol Chem 1991;266 (27):17954-8

17. Schnepf HE, Tomczak K, Ortega JP, Whiteley HR. Specificity-determining regions of a lepidopteran-specific insecticidal protein produced by *Bacillus thuringiensis*. J Biol Chem 1990;265(34):20923-30

18. Lee MK, You TH, Curtiss A, Dean DH. Involvement of two amino acid residues in the loop region of *Bacillus thuringiensis* Cry1Ab toxin in toxicity and binding to *Lymantria dispar*. Biochem Biophys Res Commun 1996;229(1):139-46

19. Lu H, Rajamohan F, Dean DH. Identification of amino acid residues of *Bacillus thuringiensis* delta-endotoxin CryIAa associated with membrane binding and toxicity to *Bombyx mori*. J Bacteriol 1994;176(17):5554-9

20. Wu SJ, Dean DH. Functional significance of loops in the receptor binding domain of *Bacillus thuringiensis* CryIIIA delta-endotoxin. J Mol Biol 1996;255(4):628-40

21. Smedley DP, Ellar DJ. Mutagenesis of three surface-exposed loops of a *Bacillus thuringiensis* insecticidal toxin reveals residues important for toxicity, receptor recognition and possibly membrane insertion. Microbiology 1996;142 (Pt 7):1617-24

22. Rajamohan F, Alcantara E, Lee MK, Chen XJ, Curtiss A, Dean DH. Single amino acid changes in domain II of *Bacillus thuringiensis* CryIAb delta-endotoxin affect irreversible binding to *Manduca sexta* midgut membrane vesicles. J Bacteriol 1995;177(9):2276-82

23. Rajamohan F, Cotrill JA, Gould F, Dean DH. Role of domain II, loop 2 residues of *Bacillus thuringiensis* CryIAb delta-endotoxin in reversible and irreversible binding to *Manduca sexta* and *Heliothis virescens*. J Biol Chem 1996;271(5):2390-6

24. Rajamohan F, Alzate O, Cotrill JA, Curtiss A, Dean DH. Protein engineering of *Bacillus thuringiensis* delta-endotoxin: mutations at domain II of CryIAb enhance receptor affinity and toxicity toward gypsy moth larvae. Proc Natl Acad Sci U S A 1996;93(25):14338-43

25. Rajamohan F, Hussain SRA, Cotrill JA, Gould F, Dean DH. Mutations at domain II, loop 3, of *Bacillus thuringiensis* CryIAa and CryIAb delta-endotoxins suggest loop 3 is involved in initial binding to lepidopteran midguts. J Biol Chem 1996;271(41):25220-6

26. Schwartz JL, Potvin L, Chen XJ, Brousseau R, Laprade R, Dean DH. Single-site mutations in the conserved alternating-arginine region affect ionic channels formed by CryIAa, a *Bacillus thuringiensis* toxin. Appl Environ Microbiol 1997;63 (10):3978-84

27. Chen XJ, Lee MK, Dean DH. Site-directed mutations in a highly conserved region of *Bacillus thuringiensis* delta-endotoxin affect inhibition of short circuit current across *Bombyx mori* midguts. Proc Natl Acad Sci U S A 1993;90(19):9041-5

28. de Maagd RA, Kwa MS, van der Klei H, Yamamoto T, Schipper B, Vlak JM, Stiekema WJ, Bosch D. Domain III substitution in *Bacillus thuringiensis* delta-endotoxin CryIA(b) results in superior toxicity for *Spodoptera exigua* and altered membrane protein recognition. Appl Environ Microbiol 1996;62(5):1537-43

29. de Maagd RA, van der Klei H, Bakker PL, Stiekema WJ, Bosch D. Different domains of *Bacillus thuringiensis* delta-endotoxins can bind to insect midgut membrane proteins on ligand blots. Appl Environ Microbiol 1996;62(8):2753-7

30. de Maagd RA, Bakker PL, Masson L, Adang MJ, Sangadala S, Stiekema W, Bosch D. Domain III of the *Bacillus thuringiensis* delta-endotoxin Cry1Ac is involved in binding to *Manduca sexta* brush border membranes and to its purified aminopeptidase N. Mol Microbiol 1999;31(2):463-71

31. Lee MK, Milne RE, Ge AZ, Dean DH. Location of a *Bombyx mori* receptor binding region on a *Bacillus thuringiensis* delta-endotoxin. J Biol Chem 1992;267 (5):3115-21

32. Lee MK, Young BA, Dean DH. Domain III exchanges of *Bacillus thuringiensis* CryIA toxins affect binding to different gypsy moth midgut receptors. Biochem Biophys Res Commun 1995;216(1):306-12

33. Carroll J, Li J, Ellar DJ. Proteolytic processing of a coleopteran-specific delta-endotoxin produced by *Bacillus thuringiensis* var. tenebrionis. Biochem J 1989;261(1):99-105

34. Lorence A, Darszon A, Bravo A. Aminopeptidase dependent pore formation of *Bacillus thuringiensis* Cry1Ac toxin on *Trichoplusia ni* membranes. FEBS Lett 1997;414(2):303-7

35. Carroll J, Wolfersberger MG, Ellar DJ. The *Bacillus thuringiensis* Cry1Ac toxin-induced permeability change in *Manduca sexta* midgut brush border membrane vesicles proceeds by more than one mechanism. J Cell Sci 1997;110 (Pt 24):3099-104

36. Escriche B, Ferre J, Silva FJ. Occurrence of a common binding site in Mamestra brassicae, Phthorimaea operculella, and *Spodoptera exigua* for the insecticidal crystal proteins CryIA from *Bacillus thuringiensis*. Insect Biochem Mol Biol 1997;27(7):651-6

37. Lee MK, You TH, Young BA, Cotrill JA, Valaitis AP, Dean DH. Aminopeptidase N purified from gypsy moth brush border membrane vesicles is a specific receptor for *Bacillus thuringiensis* CryIAc toxin. Appl Environ Microbiol 1996;62(8):2845-9

38. Luo K, Sangadala S, Masson L, Mazza A, Brousseau R, Adang MJ. The *Heliothis virescens* 170 kDa aminopeptidase functions as "receptor A" by mediating specific *Bacillus thuringiensis* Cry1A delta-endotoxin binding and pore formation. Insect Biochem Mol Biol 1997;27(8-9):735-43

39. Vadlamudi RK, Weber E, Ji I, Ji TH, Bulla LA Jr. Cloning and expression of a receptor for an insecticidal toxin of *Bacillus thuringiensis*. J Biol Chem 1995;270 (10):5490-4

40. Knowles BH, Francis PH, Ellar DJ. Structurally related *Bacillus thuringiensis* delta-endotoxins display major differences in insecticidal activity in vivo and in vitro. J Cell Sci 1986;84:221-36

41. Pasternak CA, Alder GM, Bashford CL, Korchev YE, Pederzolli C, Rostovtseva TK. Membrane damage: common mechanisms of induction and prevention. FEMS Microbiol Immunol 1992;5(1-3):83-92

42. Slatin SL, Abrams CK, English L. Delta-endotoxins form cation-selective channels in planar lipid bilayers. Biochem Biophys Res Commun 1990;169(2):765-72

43. Smedley DP, Armstrong G, Ellar DJ. Channel activity caused by a *Bacillus thuringiensis* delta-endotoxin preparation depends on the method of activation. Mol Membr Biol 1997;14(1):13-8

44. Walters FS, Slatin SL, Kulesza CA, English LH. Ion channel activity of N-terminal fragments from CryIA(c) delta-endotoxin. Biochem Biophys Res Commun 1993;196(2):921-6

45. Cummings CE, Armstrong G, Hodgman TC, Ellar DJ. Structural and functional studies of a synthetic peptide mimicking a proposed membrane inserting region of a *Bacillus thuringiensis* delta-endotoxin. Mol Membr Biol 1994;11(2):87-92

46. Ahmad W, Ellar DJ. Directed mutagenesis of selected regions of a *Bacillus thuringiensis* entomocidal protein. FEMS Microbiol Lett 1990;56(1-2):97-104

47. Wu D, Aronson AI. Localized mutagenesis defines regions of the *Bacillus thuringiensis* delta-endotoxin involved in toxicity and specificity. J Biol Chem 1992;267(4):2311-7

48. Villalon M, Vachon V, Brousseau R, Schwartz JL, Laprade R. Video imaging analysis of the plasma membrane permeabilizing effects of *Bacillus thuringiensis* insecticidal toxins in Sf9 cells. Biochim Biophys Acta 1998;1368(1):27-34

49. Carroll J, Ellar DJ. Analysis of the large aqueous pores produced by a *Bacillus thuringiensis* protein insecticide in *Manduca sexta* midgut-brush-border-membrane vesicles. Eur J Biochem 1997;245(3):797-804

50. Feng Q, Becktel WJ. pH-induced conformational transitions of Cry IA(a), Cry IA (c), and Cry IIIA delta-endotoxins in *Bacillus thuringiensis*. Biochemistry 1994;33 (28):8521-6

51. Guereca L, Bravo A. The oligomeric state of *Bacillus thuringiensis* Cry toxins in solution. Biochim Biophys Acta 1999;1429(2):342-50

52. Aronson AI, Geng C, Wu L. Aggregation of *Bacillus thuringiensis* Cry1A Toxins upon Binding to Target Insect Larval Midgut Vesicles. Appl Environ Microbiol 1999;65(6):2503-2507

53. Harvey WR, Crawford DN, Eisen NS, Fernandes VF, Spaeth DD, Wolfersberger MG. The potassium impermeable apical membrane of insect epithelia: a target for development of safe pesticides. Mem Inst Oswaldo Cruz 1987;82 Suppl 3:29-34

54. Peyronnet O, Vachon V, Brousseau R, Baines D, Schwartz JL, Laprade R. Effect of *Bacillus thuringiensis* toxins on the membrane potential of lepidopteran insect midgut cells. Appl Environ Microbiol 1997;63(5):1679-84

55. Potvin L, Laprade R, Schwartz JL. Cry1Ac, a *Bacillus thuringiensis* toxin, triggers extracellular Ca^{2+} influx and Ca^{2+} release from intracellular stores in Cf1 cells. J Exp Biol 1998;201 (Pt 12):1851-8

56. Schwartz JL, Lu YJ, Sohnlein P, Brousseau R, Laprade R, Masson L, Adang MJ. Ion channels formed in planar lipid bilayers by *Bacillus thuringiensis* toxins in the presence of *Manduca sexta* midgut receptors. FEBS Lett 1997;412(2):270-6

57. Schwartz JL, Garneau L, Savaria D, Masson L, Brousseau R, Rousseau E. Lepidopteran-specific crystal toxins from *Bacillus thuringiensis* form cation- and anion-selective channels in planar lipid bilayers. J Membr Biol 1993;132(1):53-62

58. Venugopal MG, Wolfersberger MG, Wallace BA. Effects of pH on conformational properties related to the toxicity of *Bacillus thuringiensis* delta-endotoxin. Biochim Biophys Acta 1992;1159(2):185-92

59. Hussain SR, Aronson AI, Dean DH. Substitution of residues on the proximal side of Cry1A *Bacillus thuringiensis* delta-endotoxins affects irreversible binding to *Manduca sexta* midgut membrane. Biochem Biophys Res Commun 1996;226(1):8-14

60. Uawithya P, Tuntitippawan T, Katzenmeier G, Panyim S, Angsuthanasombat C. Effects on larvicidal activity of single proline substitutions in alpha3 or alpha4 of the *Bacillus thuringiensis* Cry4B toxin. Biochem Mol Biol Int 1998;44(4):825-32

61. Wolfersberger MG, Chen XJ, Dean DH. Site-directed mutations in the third domain of *Bacillus thuringiensis* delta-endotoxin CryIAa affect its ability to increase the permeability of *Bombyx mori* midgut brush border membrane vesicles. Appl Environ Microbiol 1996;62(1):279-82

62. Gazit E, Shai Y. Structural and functional characterization of the alpha 5 segment of *Bacillus thuringiensis* delta-endotoxin. Biochemistry 1993;32(13):3429-36

63. Gazit E, Shai Y. The assembly and organization of the alpha 5 and alpha 7 helices from the pore-forming domain of *Bacillus thuringiensis* delta-endotoxin. Relevance to a functional model. J Biol Chem 1995;270(6):2571-8

64. Gazit E, Bach D, Kerr ID, Sansom MS, Chejanovsky N, Shai Y. The alpha-5 segment of *Bacillus thuringiensis* delta-endotoxin: in vitro activity, ion channel formation and molecular modelling. Biochem J 1994;304 (Pt 3):895-902

65. Biggin PC, Sansom MS. Simulation of voltage-dependent interactions of alpha-helical peptides with lipid bilayers. Biophys Chem 1996;60(3):99-110

66. Schulman BA, Kim PS. Proline scanning mutagenesis of a molten globule reveals non-cooperative formation of a protein's overall topology. Nat Struct Biol 1996;3 (8):682-7

67. Sambrook J, Maniatis T, Fritsch EF. Molecular cloning: a laboratory manual. Cold Spring Harbor laboratory 1989.

68. Chen M, Christen P. Removal of chromosomal DNA by $Mg2^{+}$ in the lysis buffer: an improved lysis protocol for preparing *Escherichia coli* whole-cell lysates for sodium dodecyl sulfate-polyacrylamide gel electrophoresis. Anal Biochem 1997;246(2):263-4

69. Laemmli UK, Molbert E, Showe M, Kellenberger E. Form-determining function of the genes required for the assembly of the head of bacteriophage T4. J Mol Biol 1970;49(1):99-113

70. Angsuthanasombat C, Crickmore N, Ellar DJ. Cytotoxicity of a cloned *Bacillus thuringiensis* subsp. israelensis CryIVB toxin to an Aedes aegypti cell line. FEMS Microbiol Lett 1991;67(3):273-6

71. Angsuthanasombat C, Crickmore N, Ellar DJ. Effects on toxicity of eliminating a cleavage site in a predicted interhelical loop in *Bacillus thuringiensis* CryIVB delta-endotoxin. FEMS Microbiol Lett 1993;111(2-3):255-61

72. Bosch D, Visser B, Stiekema WJ. Analysis of non-active engineered *Bacillus thuringiensis* crystal proteins. FEMS Microbiol Lett 1994;118(1-2):129-33

73. Meza R, Nunez-Valdez ME, Sanchez J, Bravo A. Isolation of Cry1Ab protein mutants of *Bacillus thuringiensis* by a highly efficient PCR site-directed mutagenesis system. FEMS Microbiol Lett 1996;145(3):333-9

74. Ort P, Zalunin IA, Gasparov VS, Chestukhina GG, Stepanov VM. Domain organization of *Bacillus thuringiensis* CryIIIA delta-endotoxin studied by denaturation in guanidine hydrochloride solutions and limited proteolysis. J Protein Chem 1995;14(4):241-9

APPENDIX

Appendix 1 : Complete nucleotide sequence of *cry4B* gene

The nucleotide sequence shown is the sequence of cry4B gene in pMU388. The uppercase letters represent the deduced amino acid sequence. The predicted alpha helices in domain I are marked as box.

```
atg aat tca ggc tat ccg tta gcg aat gac tta caa ggg tca atg 45
 M   N   S   G   Y   P   L   A   N   D   L   Q   G   S   M

aaa aac acg aac tat aaa gat tgg cta gcc atg tgt gaa aat aac 90
 K   N   T   N   Y   K   D   W   L   A   M   C   E   N   N

caa cag tat ggc gtt aat cca gct gcg att aat tct tct tca gtt 135
 Q   Q   Y   G   V   N   P   A   A   I   N   S   S   S   V
             Helix 1
agt acc gct tta aaa gta gct gga gct atc ctt aaa ttt gta aac 180
 S   T   A   L   K   V   A   G   A   I   L   K   F   V   N
                                 Helix 2a
cca cct gca ggt act gtc tta acc gta ctt agc gcg gtg ctt cct 225
 P   P   A   G   T   V   L   T   V   L   S   A   V   L   P

att ctt tgg ccg act aat act cca acg cct gaa aga gtt tgg aat 270
 I   L   W   P   T   N   T   P   T   P   E   R   V   W   N
       Helix 2b
gat ttc atg acc aat aca ggg aat ctt att gat caa act gta aca 315
 D   F   M   T   N   T   G   N   L   I   D   Q   T   V   T
                                                 Helix 3
gct tat gta cga aca gat gca aat gca aaa atg acg gtt gtg aaa 360
 A   Y   V   R   T   D   A   N   A   K   M   T   V   V   K

gat tat tta gat caa tat aca act aaa ttt aac act tgg aaa aga 405
 D   Y   L   D   Q   Y   T   T   K   F   N   T   W   K   R

gag cct aat aac cag tcc tat aga aca gca gta ata act caa ttt 450
 E   P   N   N   Q   S   Y   R   T   A   V   I   T   Q   F
Helix 4
aac tta acc agt gcc aaa ctt cga gag acc gca gtt tat ttt agc 495
 N   L   T   S   A   K   L   R   E   T   A   V   Y   F   S

aac tta gta ggt tat gaa tta ttg tta tta cca ata tac gca caa 540
 N   L   V   G   Y   E   L   L   L   L   P   I   Y   A   Q
Helix 5
gta gca aat ttc aat tta ctt tta ata aga gat ggc ctc ata aat 585
 V   A   N   F   N   L   L   L   I   R   D   G   L   I   N

gca caa gaa tgg tct tta gca cgt agt gct ggt gac caa cta tat 630
 A   Q   E   W   S   L   A   R   S   A   G   D   Q   L   Y
                                 Helix 6
aac act atg gtg cag tac act aaa gaa tat att gca cat agc att 675
 N   T   M   V   Q   Y   T   K   E   Y   I   A   H   S   I

aca tgg tat aat aaa ggt tta gat gta ctt aga aat aaa tct aat 720
 T   W   Y   N   K   G   L   D   V   L   R   N   K   S   N
                                                 Helix 7
gga caa tgg att acg ttt aat gat tat aaa aga gag atg act att 765
 G   Q   W   I   T   F   N   D   Y   K   R   E   M   T   I
```

```
caa gta tta gat ata ctc gct ctt ttt gcc agt tat gat cca cgt 810
 Q   V   L   D   I   L   A   L   F   A   S   Y   D   P   R

cga tac cct gcg gac aaa ata gat aat acg aaa cta tca aaa aca 855
 R   Y   P   A   D   K   I   D   N   T   K   L   S   K   T

gaa ttt aca aga gag att tat aca gct tta gta gaa tct cct tct 900
 E   F   T   R   E   I   Y   T   A   L   V   E   S   P   S

agt aaa tct ata gca gca ctg gag gca gca ctt aca cga gat gtt 945
 S   K   S   I   A   A   L   E   A   A   L   T   R   D   V

cat tta ttc act tgg cta aag aga gta gat ttc tgg acc aat act 990
 H   L   F   T   W   L   K   R   V   D   F   W   T   N   T

ata tat caa gat tta aga ttt tta tct gcc aat aaa att ggg ttt 1035
 I   Y   Q   D   L   R   F   L   S   A   N   K   I   G   F

tca tat aca aat tct tct gca atg caa gaa agt gga att tat gga 1080
 S   Y   T   N   S   S   A   M   Q   E   S   G   I   Y   G

agt tct ggt ttt ggt tca aat ctt act cat caa att caa ctt aat 1125
 S   S   G   F   G   S   N   L   T   H   Q   I   Q   L   N

tct aat gtt tat aaa act tct atc aca gat act agc tcc ccc tct 1170
 S   N   V   Y   K   T   S   I   T   D   T   S   S   P   S

aat cga gtt aca aaa atg gat ttc tac aaa att gat ggt act ctt 1215
 N   R   V   T   K   M   D   F   Y   K   I   D   G   T   L

gcc tct tat aat tca aat ata aca cca act cct gaa ggt tta agg 1260
 A   S   Y   N   S   N   I   T   P   T   P   E   G   L   R

acc aca ttt ttt gga ttt tca aca aat gag aac aca cct aat caa 1305
 T   T   F   F   G   F   S   T   N   E   N   T   P   N   Q

cca act gta aat gat tat acg cat att tta agc tat ata aaa act 1350
 P   T   V   N   D   Y   T   H   I   L   S   Y   I   K   T

gat gtt ata gat tat aac agt aac agg gtt tca ttt gct tgg aca 1395
 D   V   I   D   Y   N   S   N   R   V   S   F   A   W   T

cat aag att gtt gac cct aat aat caa ata tac aca gat gct atc 1440
 H   K   I   V   D   P   N   N   Q   I   Y   T   D   A   I

aca caa gtt ccg gcc gta aaa tct aac ttc ttg aat gca aca gct 1485
 T   Q   V   P   A   V   K   S   N   F   L   N   A   T   A

aaa gta atc aag gga cct ggt cat aca ggg ggg gat cta gtt gct 1530
 K   V   I   K   G   P   G   H   T   G   G   D   L   V   A

ctt aca agc aat ggt act cta tca ggc aga atg gag att caa tgt 1575
 L   T   S   N   G   T   L   S   G   R   M   E   I   Q   C

aaa aca agt att ttt aat gat cct aca aga agt tac gga tta cgc 1620
 K   T   S   I   F   N   D   P   T   R   S   Y   G   L   R

ata cgt tat gct gca aat agt cca att gta ttg aat gta tca tat 1665
 I   R   Y   A   A   N   S   P   I   V   L   N   V   S   Y

gta tta caa gga gtt tct aga gga aca acg att agt aca gaa tct 1710
 V   L   Q   G   V   S   R   G   T   T   I   S   T   E   S

acg ttt tca aga cct aat aat ata ata cct aca gat tta aaa tat 1755
 T   F   S   R   P   N   N   I   I   P   T   D   L   K   Y
```

```
gaa gag ttt aga tac aaa gat cct ttt gat gca att gta ccg atg 1800
 E   E   F   R   Y   K   D   P   F   D   A   I   V   P   M

aga tta tct tct aat caa ctg ata act ata gct att caa cca tta 1845
 R   L   S   S   N   Q   L   I   T   I   A   I   Q   P   L

aac atg act tca aat aat caa gtg att att gac aga atc gaa att 1890
 N   M   T   S   N   N   Q   V   I   I   D   R   I   E   I

att cca atc act caa tct gta tta gat gag aca gag aac caa aat 1935
 I   P   I   T   Q   S   V   L   D   E   T   E   N   Q   N

tta gaa tca gaa cga gaa gtt gtg aat gca ctg ttt aca aat gac 1980
 L   E   S   E   R   E   V   V   N   A   L   F   T   N   D

gcg aaa gat gca tta aac att gga acg aca gat tat gac ata gat 2025
 A   K   D   A   L   N   I   G   T   T   D   Y   D   I   D

caa gcc gca aat ctt gtg gaa tgt att tct gaa gaa tta tat cca 2070
 Q   A   A   N   L   V   E   C   I   S   E   E   L   Y   P

aaa gaa aaa atg ctg tta tta gat gaa gtt aaa aat gcg aaa caa 2115
 K   E   K   M   L   L   L   D   E   V   K   N   A   K   Q

ctt agt caa tct cga aat gta ctt caa aac ggg gat ttt gaa tcg 2160
 L   S   Q   S   R   N   V   L   Q   N   G   D   F   E   S

gct acg ctt ggt tgg aca aca agt gat aat atc aca att caa gaa 2205
 A   T   L   G   W   T   T   S   D   N   I   T   I   Q   E

gat gat cct att ttt aaa ggg cat tac ctt cat atg tct ggg gcg 2250
 D   D   P   I   F   K   G   H   Y   L   H   M   S   G   A

aga gac att gat ggt acg ata ttt ccg acc tat ata ttc caa aaa 2295
 R   D   I   D   G   T   I   F   P   T   Y   I   F   Q   K

att gat gaa tca aaa tta aaa ccg tat aca cgt tac cta gta agg 2340
 I   D   E   S   K   L   K   P   Y   T   R   Y   L   V   R

gga ttt gta gga agt agt aaa gat gta gaa cta gtg gtt tca cgc 2385
 G   F   V   G   S   S   K   D   V   E   L   V   V   S   R

tat ggg gaa gaa att gat gcc atc atg aat gtt cca gct gat tta 2430
 Y   G   E   E   I   D   A   I   M   N   V   P   A   D   L

aac tat ctg tat cct tct acc ttt gat tgt gaa ggg tct aat cgt 2475
 N   Y   L   Y   P   S   T   F   D   C   E   G   S   N   R

tgt gag acg tcc gct gtg ccg gct aac att ggg aac act tct gat 2520
 C   E   T   S   A   V   P   A   N   I   G   N   T   S   D

atg ttg tat tca tgc caa tat gat aca ggg aaa aag cat gtc gta 2565
 M   L   Y   S   C   Q   Y   D   T   G   K   K   H   V   V

tgt cag gat tcc cat caa ttt agt ttc act att gat aca ggg gca 2610
 C   Q   D   S   H   Q   F   S   F   T   I   D   T   G   A

tta gat aca aat gaa aat ata ggg gtt tgg gtc atg ttt aaa ata 2655
 L   D   T   N   E   N   I   G   V   W   V   M   F   K   I

tct tct cca gat gga tac gca tca tta gat aat tta gaa gta att 2700
 S   S   P   D   G   Y   A   S   L   D   N   L   E   V   I

gaa gaa ggg cca ata gat ggg gaa gca ctg tca cgc gtg aaa cac 2745
 E   E   G   P   I   D   G   E   A   L   S   R   V   K   H
```

```
atg gag aag aaa tgg aac gat caa atg gaa gca aaa cgt tcg gaa 2790
 M   E   K   K   W   N   D   Q   M   E   A   K   R   S   E

aca caa caa gca tat gat gta gcg aaa caa gcc att gat gct tta 2835
 T   Q   Q   A   Y   D   V   A   K   Q   A   I   D   A   L

ttc aca aat gta caa gat gag gct tta cag ttt gat acg aca ctc 2880
 F   T   N   V   Q   D   E   A   L   Q   F   D   T   T   L

gct caa att cag tac gct gag tat ttg gta caa tcg att cca tat 2925
 A   Q   I   Q   Y   A   E   Y   L   V   Q   S   I   P   Y

gtg tac aat gat tgg ttg tca gat gtt cca ggt atg aat tat gat 2970
 V   Y   N   D   W   L   S   D   V   P   G   M   N   Y   D

atc tat gta gag ttg gat gca cga gtg gca caa gcg cgt tat ttg 3015
 I   Y   V   E   L   D   A   R   V   A   Q   A   R   Y   L

tat gat aca aga aat att att aaa aat ggt gat ttt aca caa ggg 3060
 Y   D   T   R   N   I   I   K   N   G   D   F   T   Q   G

gta atg ggg tgg cat gta act gga aat gca gac gta caa caa ata 3105
 V   M   G   W   H   V   T   G   N   A   D   V   Q   Q   I

gat ggt gtt tct gta ttg gtt cta tct aat tgg agt gct ggc gta 3150
 D   G   V   S   V   L   V   L   S   N   W   S   A   G   V

tct caa aat gtc cat ctc caa cat aat cat ggg tat gtc tta cgt 3195
 S   Q   N   V   H   L   Q   H   N   H   G   Y   V   L   R

gtt att gcc aaa aaa gaa gga cct gga aat ggg tat gtc acg ctt 3240
 V   I   A   K   K   E   G   P   G   N   G   Y   V   T   L

atg gat tgt gag gag aat caa gaa aaa ttg acg ttt acg tct tgt 3285
 M   D   C   E   E   N   Q   E   K   L   T   F   T   S   C

gaa gaa gga tat att acg aag aca gta gat gta ttc cca gat aca 3330
 E   E   G   Y   I   T   K   T   V   D   V   F   P   D   T

gat cgt gta cga att gag ata ggc gaa acc gaa ggt tcg ttt tat 3375
 D   R   V   R   I   E   I   G   E   T   E   G   S   F   Y

atc gaa agc att gaa tta att tgc atg aac gag                3408
 I   E   S   I   E   L   I   C   M   N   E
```

Appendix 2 : Physical maps of pMU388

The pMU388 is a plasmid carries full-length of *cry4B* gene.

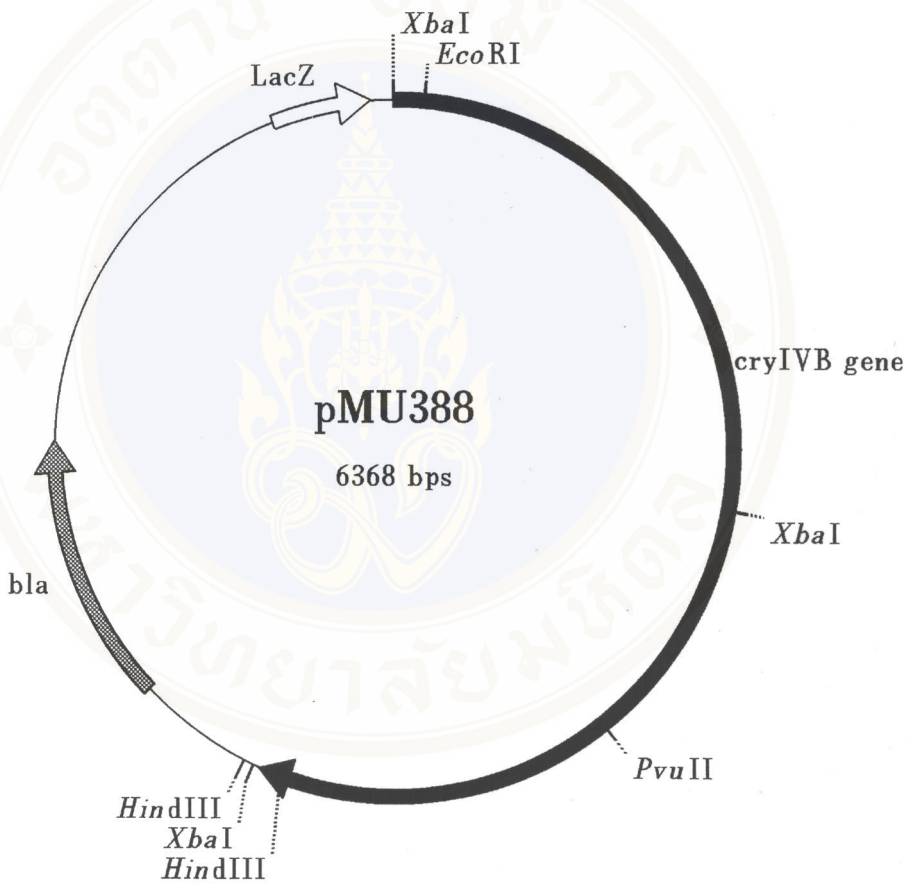

Appendix 3 : Sequences of the mutant plasmids

The CLUSTAL W(1.60) multiple sequence alignment of the sequences of the wild type pMu388 and its mutant plasmids. The boldface letters represent the mutated residues.

```
pMU388          GCAGTTTATTTTAGCAACTTAGTAGGTTATGAATTATTGTTATTACCAATATACGCACAA
A182P           GCAGTTTATTTTAGCAACTTAGTAGGTTATGAATTATTGTTATTACCAATATACGCACAG
L186P           GCNGTTTATNTNANCAACTTAGTAGGTTATGAATTATTGTTATTACCAATATACGCACAA
Y220P           ------------------TTAGTAGGTTATGAATTATTGTTATTACCAATATACGCACAA
I221P           -----TTATTT-AGCAACTTAGTAGGTTATGAATTATTGTTATTACCAATATACGCACAA
T254P           GCAGTTTATTTTAGCAACTTAGTAGGTTATGAATTATTGTTATTACCAATATACGCACAA
V257P           GCAGTTTATTTTAGCAACTTAGTAGGTTATGAATTATTGTTATTACCAATATACGCACAA

pMU388          GTAGCAAATTTCAATTTACTTTTAATAAGAGATGGCCTCATAAATGCACAAGAATGGTCT
A182P           GTCCCAAATTTCAATTTACTTTTAATAAGAGATGGCCTCATAAATGCACAAGAATGGTCT
L186P           GTAGCAAATTTCAATCCACTTTTAATCCGGGATGGCCTCATAAATGCACAAGAATGGTCT
Y220P           GTAGCAAATTTCAATTTACTTTTAATAAGAGATGGCCTCATAAATGCACAAGAATGGTCT
I221P           GTAGCAAATTTCAATTTACTTTTAATAAGAGATGGCCTCATAAATGCACAAGAATGGTCT
T254P           GTAGCAAATTTCAATTTACTTTTAATAAGAGATGGCCTCATAAATGCACAAGAATGGTCT
V257P           GTAGCAAATTTCAATTTACTTTTAATAAGAGATGGCCTCATAAATGCACAAGAATGGTCT

pMU388          TTAGCACGTAGTGCTGGTGACCAACTATATAACACTATGGTGCAGTACACTAAAGAATAT
A182P           TTAGCACGTAGTGCTGGTGACCAACTATATAACACTATGGTGCAGTACACTAAAGAATAT
L186P           TTAGCACGTAGTGCTGGTGACCAACTATATAACACTATGGTGCAGTACACTAAAGAATAT
Y220P           TTAGCACGTAGTGCTGGTGACCAACTATATAACACTATGGTGCAGTACACTAAAGAACCT
I221P           TTAGCACGTAGTGCTGGTGACCAACTATATAACACTATGGTGCAGTACACTAAAGAATAT
T254P           TTAGCACGTAGTGCTGGTGACCAACTATATAACACTATGGTGCAGTACACTAAAGAATAT
V257P           TTAGCACGTAGTGCTGGTGACCAACTATATAACACTATGGTGCAGTACACTAAAGAATAT

pMU388          ATTGCACATAGCATTACATGGTATAATAAAGGTTTAGATGTACTTAGAAATAAATCTAAT
A182P           ATTGCACATAGCATTACATGGTATAATAAAGGTTTAGATGTACTTAGAAATAAATCTAAT
L186P           ATTGCACATAGCATTACATGGTATAATAAAGGTTTAGATGTACTTAGAAATAAATCTAAT
Y220P           ATTGCGCATAGCATTACATGGTATAATAAAGGTTTAGATGTACTTAGAAATAAATCTAAT
I221P           CCTGCGCATAGCATTACATGGTATAATAAAGGTTTAGATGTACTTAGAAATAAATCTAAT
T254P           ATTGCACATAGCATTACATGGTATAATAAAGGTTTAGATGTACTTAGAAATAAATCTAAT
V257P           ATTGCACATAGCATTACATGGTATAATAAAGGTTTAGATGTACTTAGAAATAAATCTAAT

pMU388          GGACAATGGATTACGTTTAATGATTATAAAAGAGAGATGACTATTCAAGTATTAGATATA
A182P           GGACAATGGATTACGTTTAATGATTATAAAAGAGAGATGACTATTCAAGTATTAGATATA
L186P           GGACAATGGATTACGTTTAATGATTATAAAAGAGAGATGACTATTCAAGTATTAGATATA
Y220P           GGACAATGGATTACGTTTAATGATTATAAAAGAGAGATGACTATTCAAGTATTAGATATA
I221P           GGACAATGGATTACGTTTAATGATTATAAAAGAGAGATGACTATTCAAGTATTAGATATA
T254P           GGACAATGGATTACGTTTAATGATTATAAAAGAGAGATGCCGATTCAAGTATTAGATATA
V257P           GGACAATGGATTACGTTTAATGATTATAAAAGAGAGATGACTATTCAACCTCTAGATATA

pMU388          CTCGCTCTTTTTGCCAGTTATGATCCACGTCGATACCCTGCGGACAAAATAGATAATACG
A182P           CTCGCTCTTTTTGCCAGTTATGATCCACGTCGATACCCTGCGGACAAAATAGATAATACG
L186P           CTCGCTCTTTTTGCCAGTTATGATCCACGTCGATACCCTGCGGACAAAATAGATAATACG
Y220P           CTCGCTCTTTTTGCCAGTTATGATCCACGTCGATACCCTGCGGACAAAATAGATAATACG
I221P           CTCGCTCTTTTTGCCAGTTATGATCCACGTCGATACCCTGCGGACAAAATAGATAATACG
T254P           CTCGCTCTTTTTGCCAGTTATGATCCACGTCGATACCCTGCGGACAAAATAGATAATACG
V257P           CTCGCTCTTTTTGCCAGTTATGATCCACGTCGATACCCTGCGGACAAAATAGATAATACG

pMU388          AAACTATCAAAAACAGAATTTACAAGAGAGATTTATACAGCTTTAGTAGAATCTCCTTCT
A182P           AAACTATCAAAAACAGAATTTACAAGAGAGATTTATACAGCTTTAGTAGAATCTCCTTCT
L186P           AAACTATCAAAAACAGAATTTACAAGAGAGATTTATACAGCTTTAGTAGAATCTCCTTCT
Y220P           AAACTATCAAAAACAGAATTTACAAGAGAGATTTATACAGCTTTAGTAGAATCTCCTTCT
I221P           AAACTATCAAAAACAGAATTTACAAGAGAGATTTATACAGCTTTAGTAGAATCTCCTTCT
T254P           AAACTATCCAAAACAGAATTTACAAGAGAGATTTATACGGCTTTAGTAGAATCTCCTTCT
V257P           AAACTATCCAAAACAGAATTTACAAGAGAGATTTATACGGCTTTAGTAGAATCTCCTTCT
```

BIOGRAPHY

NAME Mr. Issara Sramala

DATE OF BIRTH 6 May 1976

PLACE OF BIRTH Los Angeles, CA, USA

INSTITUTIONS ATTENDED

Chulalongkorn University, 1993-1996:

Bachelor of Science (Microbiology)

Mahidol University, 1997-1999:

Master of Science (Molecular Genetics and Genetic Engineering)

RESEARCH GRANTS

Graduate Fellowship Program National Science and Technology Development Agency (NSTDA)